Chapter 3

Deposition of TiO_2 thin films using liquid phase deposition method and their site-selective depositions

3.1 Introduction

Crystalline thin films have been prepared by high temperature sintering. Fabrication processes of crystalline thin films in an aqueous solution are thus reqired. Site-selective depositions of their films are also needed to apply them for nano/micro devices. We proposed several novel processes for site-selevtive deposition of crystalline anatase TiO_2 thin films inan aqueous solution. Additionally, deposition mechanism of the films was investigated.

In chapter 3.3, we used a quartz crystal microbalance (QCM) to evaluate in detail the process by which anatase TiO_2 is deposited from an aqueous solution and developed a novel method to realize SSD of thin films using a seed layer. In chapter 3.4, site-selective immersion was realized using a SAM having a pattern of hydrophilic and hydrophobic surfaces alike. In the experiment the solution containing Ti precursor contacted the hydrophilic surface, and briefly came in contact with the hydrophobic surface via our new method. In chapter 3.5, we developed a novel method to realize site-selective deposition of thin films using a site-selective elimination method. The concept of this method is the use of the difference in adhesion strength of the depositions to the substrate. In chapter 3.6, we evaluated in detail the deposition process of anatase TiO_2 from an aqueous solution.

3.2 Experimental procedure

SAM preparation.

Octadecyltrichlorosilane (OTS-SAM) and PTCS-SAM were prepared by immersing the Si substrate (p-type Si [100]) in an anhydrous toluene solution containing 1 vol% OTS or PTCS, respectively, for 5 min under an N_2 atmosphere.[1] APTS (3-Aminopropyltriethoxysilane)-SAM was prepared by immersion in an anhydrous toluene solution containing 1 vol% APTS for 1 h in air. The substrates with SAMs were baked at 120 ℃ for 5 min to remove residual solvent and promote chemisorption of the SAM. Octadecylmercaptan (OM)-SAM, phenylmercaptan (PM)-SAM and 2-aminoethanethiol (AET)-SAM were prepared by immersing the Au-coated quartz crystal of a quartz crystal microbalance (QCM; QCA917, Seiko EG&G Co., Ltd.) in a bicyclohexyl solution containing 1 vol% OM, PM or AET, respectively, for 30 min under an N_2 atmosphere. The substrates with SAMs were then rinsed with anhydrous toluene to remove residual

reagents. OM-SAM on the quartz crystal of the QCM was exposed for 2 h to UV light (184.9 nm) to assess the deposition rate of TiO_2 on OH groups.

OTS-SAM has a methyl group at the end of a long methylene chain, whereas PTCS-SAM and APTS-SAM have phenyl groups and amino groups, respectively. OM-SAM, PM-SAM and AET-SAM have octadecyl, phenyl and amino groups, respectively, and their functional groups are similar to those of OTS-SAM, PTCS-SAM and APTS-SAM. They were used instead of OTS-SAM, PTCS-SAM or APTS-SAM for QCM analysis because trichlorosilane reagents such as OTS, PTCS and APTS cannot form SAMs on Au-coated substrates. Initially deposited OTS-SAM, PTCS-SAM, APTS-SAM, OM-SAM, PM-SAM and AET-SAM showed water contact angles of 96 °, 74 °, 48 ° 96 °, 76 ° and 53 °, respectively. UV-irradiated surfaces of SAMs were, however, wetted completely (contact angle < 5°). This suggests that SAMs of OTS, PTCS, APTS, OM, PM and AET were modified to hydrophilic OH group surfaces by UV irradiation. The order of SAM hydrophobicity determined from these measurements was OTS-SAM > PTCS-SAM > APTS-SAM > OH groups on silicon. Zeta potentials measured in aqueous solutions (pH = 7.0) for the surface of silicon substrate covered with OH groups, phenyl groups (PTCS) and amino groups (APTS) were measured to be –38.23 mV, +0.63 mV and +22.0 mV^2, respectively. The order of zeta potential in the aqueous solution of our experiment is presumed to be APTS-SAM > PTCS-SAM > OH-SAM (OH groups on silicon).

Hydrolysis of TDD and formation of amorphous TiO_2 thin films.

Patterned OTS-SAM was immersed in an anhydrous toluene (99.8 %, water < 0.002 %, Aldrich) solution containing 0.1 M TDD for 30 min under an N_2 atmosphere using a glove box. All glassware was dried in a dry box at 50 ºC before use. The estimated partial pressure of H_2O in an N_2 atmosphere is below 0.1 hPa. Chlorine atoms of TDD react with H_2O and change into OH, which further react with silanol groups of SAM resulting in the formation of Ti-O-Si bonds.[3] The ethoxy group, OC_2H_5, of TDD is hydrolyzed into hydroxyl groups which are further condensed to form Ti-O-Ti bonds.[3] The thickness of films can be easily controlled by varying the soaking time. After SAM substrates had been rinsed with toluene and preserved in air, thin films appeared on the silanol surfaces of OTS-SAM but were not observed on octadecyl surfaces. A micropattern of amorphous TiO_2 thin films was thus fabricated on a patterned OTS-SAM. Additionally, OM-SAM was formed on the Au-coated quartz crystal and then modified to a hydroxyl group surface (OH-SAM) by UV irradiation. A quartz crystal covered by hydroxyl groups was immersed in the TDD solution to form amorphous TiO_2 thin film, and was used for quantitative analysis by a QCM.

Deposition of anatase TiO_2 thin films.

Ammonium hexafluorotitanate ($[NH_4]_2TiF_6$) (purity 96 %, 1.031 g) and boric acid (H_3BO_3) (purity 99.5 %, 0.932 g) were dissolved separately in deionized water (50 °C, 50 ml) (Fig. 1). An appropriate amount of HCl was added to the boric acid solution to control pH, and ammonium hexafluorotitanate solution was added.[1] Solutions (100 ml) with 0, 0.1 or 0.6 ml of HCl showed pH 3.8, 2.8 or 1.5, respectively. SAMs were immersed in the solution (100 ml) containing 0.05 M $(NH_4)_2TiF_6$ and 0.15 M (H_3BO_3) at pH 1.5, 2.8 or 3.8 and kept at 50 °C to deposit anatase TiO_2. Deposition of TiO_2 proceeded by the following mechanism[4-6]:

$$TiF_6^{2-} + 2H_2O \rightleftharpoons TiO_2 + 4H^+ + 6F^- \quad \cdots(a)$$

$$BO_3^{3-} + 4F^- + 6H^+ \longrightarrow BF_4^- + 3H_2O \quad \cdots(b)$$

Equation (a) is described in detail by the following two equations:

$$TiF_6^{2-} \xrightarrow{nOH^-} TiF_{6-n}(OH)_n^{2-} + nF^- \xrightarrow{(6-n)OH^-} Ti(OH)_6^{2-} + 6F^- \quad \cdots(c)$$

$$Ti(OH)_6^{2-} \xrightarrow{H_2O} TiO_2 \quad \cdots(d)$$

Fluorinated titanium complex ions gradually change into titanium hydroxide complex ions in an aqueous solution as shown in Eq. (c). Anatase TiO_2 was formed from titanium hydroxide complex ions ($Ti(OH)_6^{2-}$) in Eq. (d), and thus the supersaturation degree and the deposition rate of TiO_2 depend on the concentration of titanium hydroxide complex ions. The high concentration of H^+ displaces the equilibrium to the left in Eq. (a), and the low concentration of OH^-, which is replaced with F^- ions, suppresses ligand exchange in Eq. (c) and decreases the concentration of titanium hydroxide complex ions at low pH such as pH 1.5. The solution actually remained clear at pH 1.5, showing its low degree of supersaturation. On the other hand, the solution at high pH such as pH 2.8 or 3.8 became turbid because of homogeneously-nucleated anatase TiO_2 particles caused by a high degree of supersaturation. Anatase TiO_2 thin film was formed by heterogeneous nucleation in the solution at pH 1.5, while the film was formed by heterogeneous nucleation and deposition of homogeneously nucleated particles at pH 2.8 or 3.8.

QCM measurement.

Quartz crystals covered with SAMs were placed 5 mm below the surface of the solution. The solution was kept covered to prevent the evaporation of water, and water (50 °C) was added to compensate for any evaporated water. Frequency decrease (ΔF (Hz)) was converted into weight increase (Δm (ng)) by the following equation:

$$\Delta m\,(ng) = -1.068 \times \Delta F(Hz) \cdots (c)$$

References

(1) Koumoto, K., Seo, S., Sugiyama, T., Seo, W.S. and Dressick, W.J. *J. Chem. Mater.* **1999**, *11(9)*, 2305.

(2) Zhu, P. X.; Ishikawa, M.; Seo, W. S.; Koumoto, K. *J. Biomed. Mater. Res.* **2002**, *59*, 294-304.

(3) Lee, L. H. *J. Colloid Interface Sci.* **1968**, *27*, 751.

(4) Deki, S., Aoi, Y., Hiroi, O. and Kajinami, A. *Chem. Lett.* **1996**, 433-434.

(5) Deki, S., Aoi, Y., Yanagimoto, H., Ishii, K., Akamatsu, K., Mizuhata, M. and Kajinami, A. *J. Mater. Chem.* **1996**, *6*, 1879-1882.

(6) Deki, S., Aoi, Y., Asaoka, Y., Kajinami, A. and Mizuhata, M. *J. Mater. Chem.* **1997**, *7*, 733-736.

3.3 Site-selective deposition of anatase TiO_2 thin films in an aqueous solution using a seed layer

We used a quartz crystal microbalance (QCM) to evaluate in detail the process by which anatase TiO_2 is deposited from an aqueous solution and developed a novel method to realize SSD of thin films using a seed layer.

Quantitative analysis of the deposition of anatase TiO_2 onto an amorphous TiO_2 thin film or onto SAMs. Quartz crystals covered with amorphous TiO_2 thin film, OM-SAM (CH_3), PM-SAM (Ph), AET-SAM (NH_2) or OH-SAM (OH) were immersed in a solution containing 0.05 M TiF_6^{2-} and 0.015 M BO_3^{3-} at pH 1.5 or pH 2.8 (Fig. 1). The supersaturation degree of the solution at pH 1.5 was low as the high concentration of H^+ suppressed TiO_2 generation in equation (a), and hence the deposition reaction progresses slowly with no homogeneous nucleation occurring in the solution. We found that anatase TiO_2 was deposited on an amorphous TiO_2 thin film faster than on OM-, PM- AET- or OH-SAMs at pH 1.5. This shows that the deposition of anatase TiO_2 was accelerated on amorphous TiO_2 compared with on silanol, amino, phenyl or octadecyl groups. Amorphous TiO_2 probably decreases the nucleation energy of anatase TiO_2. The difference in deposition rate enables SSD to be achieved. The amorphous TiO_2 thin film can be

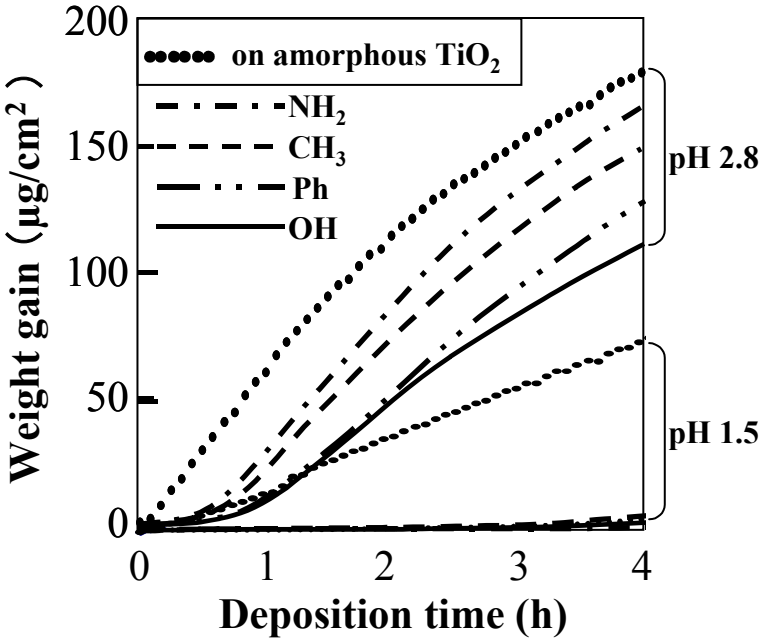

Figure 1. Deposition quantity of anatase TiO_2 on amorphous TiO_2, octadecyl groups, phenyl groups, amino groups or hydroxyl groups at (a) pH 1.5 or (b) pH 2.8 as a function of deposition time.

used as a seed layer to accelerate the deposition of anatase TiO_2. The deposition rate at pH 2.8 was larger than that at pH 1.5 because of the high degree of supersaturation, and homogeneously nucleated particles in the solution deposited on the whole surface of the substrate, regardless of the surface functional groups. The thickness of anatase TiO_2 thin film deposited on a quartz crystal covered with amorphous TiO_2 at pH 1.5 for 1 h and at pH 2.8 for 30 min was estimated to be 36 nm and 76 nm, respectively, assuming the density of anatase type TiO_2 to be 3.89 g/cm^3.

Patterning of OTS-SAM and SSD of amorphous TiO_2. OTS-SAM was prepared on a silicon substrate. The calculation was performed at the Hartree-Fock/3-21G(*) level utilizing the Spartan program (SPARTAN '02 for Windows, Wavefunction, Inc.)[1] to optimize the geometry of the OTS molecule. The distance between the hydrogen atom at the end of the molecule and silicon was calculated to be 2.43 nm and this will be the thickness of OTS-SAM. OTS-SAM was modified by UV irradiation to give rise to a micropattern with silanol/octadecyl groups (Fig. 2) and was observed with a scanning electron microscope (SEM; S-3000N, Hitachi Ltd.). Silanol regions showed white contrast in SEM micrographs (Fig. 3 (1-a), (1-b)) compared with non-UV irradiated regions. In general, high area shows it white compared with low area. However, high areas such as OTS-SAM regions appeared black compared with low silanol regions. SEM contrast is affected by many factors. The amorphous SiO_2 layer on the surface of a silicon wafer probably emits many secondary electrons compared with OTS-SAM, and OTS-SAM inhibits the emission of secondary electrons from under the amorphous SiO_2 layer. Hence, the regions covered by OTS-SAM appeared black compared with silanol group regions. This phenomenon was also observed with patterned

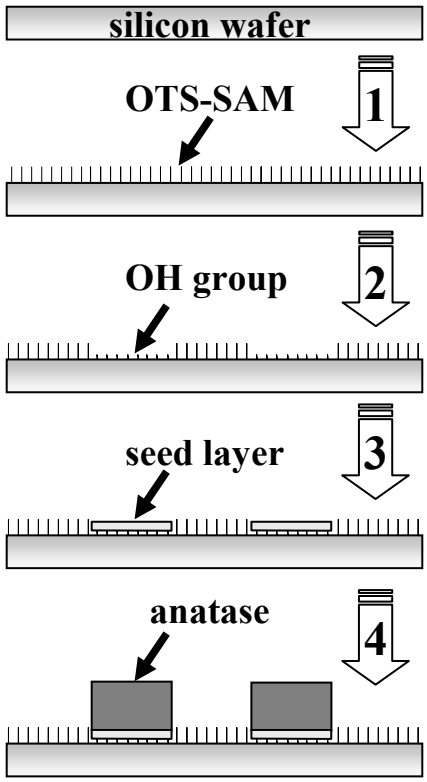

Figure 2. Schematic for SSD of anatase TiO_2 thin films using a seed layer.
Process sequence = 1- SAM Preparation; 2- Patterned UV Irradiation; 3- Site-selective Amorphous TiO_2 Seed Deposition on Silanols; 4- Site-selective Anatase Deposition on Amorphous TiO_2 Seed Regions.

PTCS-SAM and APTS-SAM.[2] The patterned SAM was further immersed in the solution containing TDD molecules for 30 min.[3] Amorphous TiO_2 was selectively deposited on silanol regions and showed black contrast in SEM micrographs (Fig. 3 (2-a), (2-b)) compared with non-UV irradiated regions.[3] Amorphous TiO_2 deposited from our solution probably emits fewer secondary electrons compared with the amorphous SiO_2 layer on the surface of a silicon wafer, and the TiO_2 layer would inhibit the emission of secondary electrons from under the amorphous SiO_2 layer. This probably causes the contrast in Fig. 3 (2-a), (2-b). The line edge roughness was estimated with the same manner as we used for titanium dioxide films.[3-4] Line width measurements at 15 equally spaced points on each line indicate an average printed line width of 23.3 μm. Line edge roughness, as measured by the standard deviation of the line width, is ~ 0.5 μm. This represents an ~ 2.1 % variation (i.e., 0.5 / 23.2) in the nominal line width. X-ray diffraction measurements (XRD) (Rigaku RU-200) with CuKα radiation (40 kV, 30 mA) for as-deposited thin films showed that they were composed of amorphous phases.[3] The ratio of oxygen to titanium was evaluated after 20 min of Ar^+ ion sputtering to avoid the influence of the contaminated layer on the surface.[3] The 1s peak of O can be deconvoluted into two curves (ratio of 529.7 eV (films) and 531.3 eV (silicon oxide) is 1 : 0.22). The ratio of oxygen to titanium was estimated to be 2.2 : 1. Small amounts of chlorine and carbon were also detected (Ti : O : Cl : C = 1 : 2.2 : 0.17 : 0.37).[21]

SSD of anatase TiO_2 on a seed layer. A micropattern having amorphous TiO_2 and octadecyl groups was immersed in an aqueous solution at pH 1.5 for 1 h (Fig. 2). Deposited thin films made it appear white compared with octadecyl group regions in SEM micrographs (Fig. 3 (3-a), (3-b)) because of the difference in height. The feature edge acuity of antase TiO_2 pattern was ~ 2.1 % variation (i.e., 0.5 / 23.2) and was much the same as we calculated from amorphous TiO_2 pattern. This resemblance was observed from Fig 2-a and 3-a. These micrographs were taken from the same position. Variations of these patterns were much better than that of the pattern fabricated with a lift-off process[4] and the usual 5 % variation afforded by current electronics design rules. Additionally, these variations were similar to that of a TEM mesh (2.1 %) we used for Fig. 3. Therefore, variations of these patterns can be improved through the use of a high resolution photomask. Site-selective deposition was also possible for the 2h or 3h reaction. However, TiO_2 began to deposit on OTS regions gradually after 4h soaking. Homogeneously nucleated particles were deposited on the whole area of the substrate (Fig. 3-a) but these particles can be removed easily by ultrasonication. The thin films were evaluated by an X-ray diffractometer (XRD; RAD-C, Rigaku) with CuKα radiation (40 kV, 30 mA) and Ni filter plus a graphite monochromater. Deposited films showed weak XRD patterns of anatase type TiO_2 because the films were not sufficiently thick to show strong diffraction. This finding

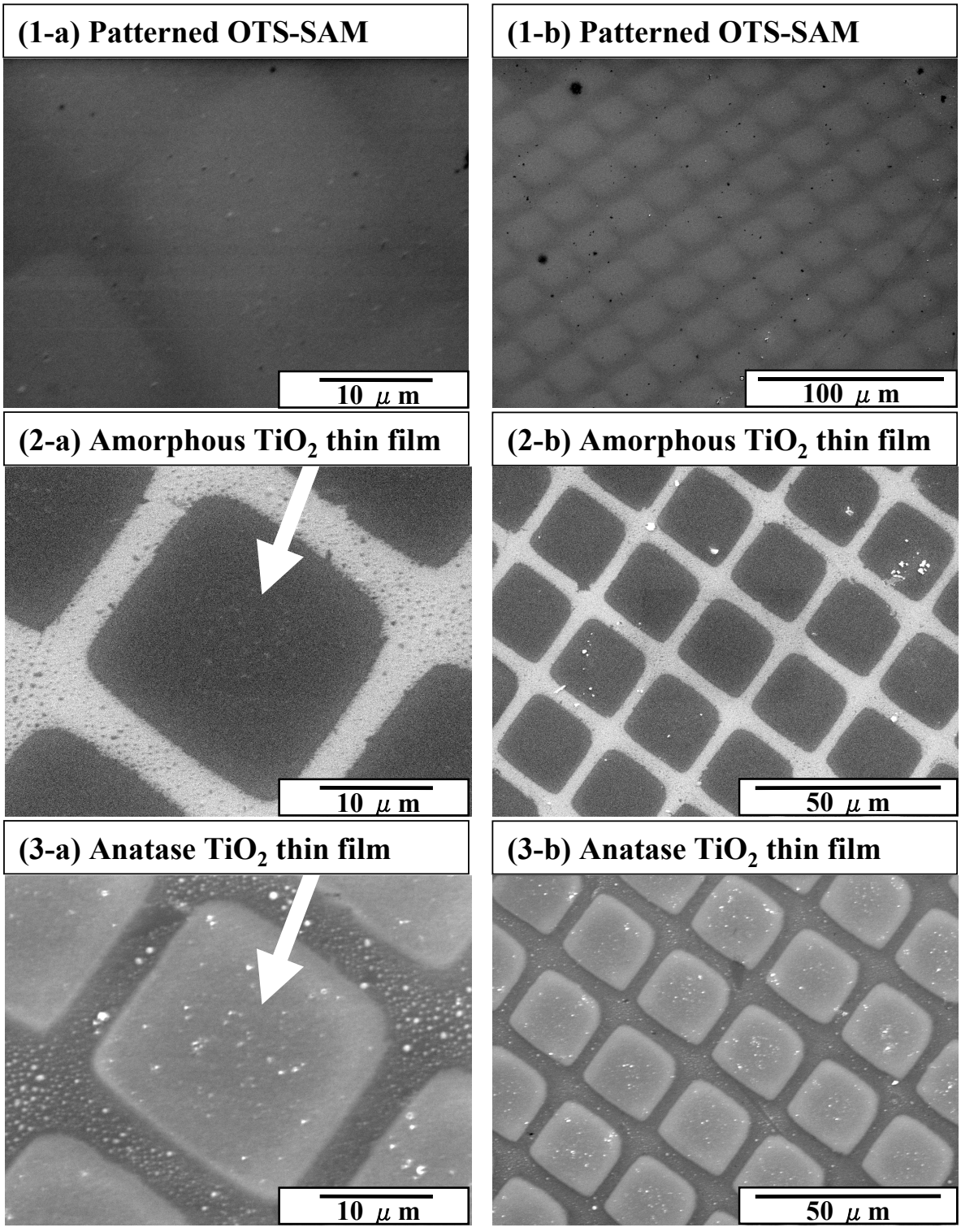

Figure 3. SEM micrographs of (1-a), (1-b) patterned OTS-SAM, (2-a), (2-b) a micropattern of amorphous TiO_2 thin films and (3-a), (3-b) a micropattern of anatase TiO_2 thin films deposited at pH 1.5.

provides evidence for the deposition of anatase TiO_2 on amorphous TiO_2 regions. An atomic force microscope (AFM; Nanoscope E, Digital Instruments) image showed anatase TiO_2 thin films to be higher than octadecyl group regions (Fig. 4). The center of the anatase TiO_2 thin film region was 61 nm higher than the octadecyl regions, and the thickness of the anatase TiO_2 thin film was estimated to be 36 nm considering the thickness of amorphous TiO_2 thin film (27 nm)[2] and OTS molecules (2.4 nm) (Fig. 2). This result is similar to that estimated by QCM measurement (36 nm). The surface roughness (RMS) of the anatase TiO_2 thin film was estimated using an AFM image and the equation:

$$\text{RMS (standard deviation)} = [\Sigma_i (Z_i - Z_{ave})^2 / n]^{1/2} \quad \cdots(e)$$

Z_i: height at point i, Z_{ave}: average of Z (height), n: number of data points.

The AFM image showed the film roughness to be 3.7 nm (horizontal distance between measurement points: 6.0 μm) (Fig. 4-(a)), which is less than that of amorphous TiO_2 thin film (RMS 9.7 nm, 27 nm thick, horizontal distance between measurement points: 6.0 μm)).[2] Additionally, the roughness of the octadecyl group regions was shown to be 0.63 nm (horizontal distance between measurement points: 1.8 μm) (Fig. 4-(b)).

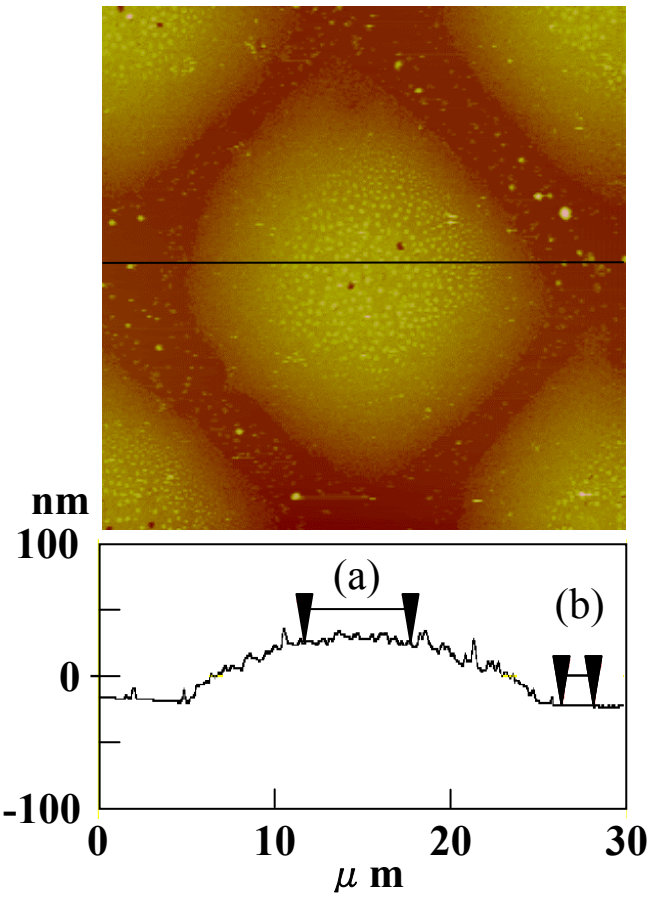

Figure 4. AFM image, cross section profile and (a), (b) measurement areas of surface roughness of a micropattern of anatase TiO_2 thin films deposited at pH 1.5.

Amorphous TiO_2 accelerated the deposition of anatase TiO_2 and showed its excellent performance as a seed layer. The feature edge acuity of anatase TiO_2 patterns was estimated to be approximately 2.1 % using the same method as used for a micropattern fabricated by the lift-off process[4] and was the same as that of amorphous TiO_2.[3] The feature edge acuity could be improved by using a higher feature edge acuity photomask since this variance is similar to that of the TEM mesh (2.1 %). XRD measurements for the thin film deposited for 1 h did not show any peaks since the deposited quantity was not sufficient to show any diffraction, however, the thin film deposited for 7 h was composed of anatase TiO_2. Anatase TiO_2 thin films were not peeled off by sonication in ethanol for 10 min and showed strong adhesion to the amorphous TiO_2 layer. This suggests that strong chemical bonds were formed between anatase TiO_2 and amorphous TiO_2.

Deposition of anatase TiO_2 in an aqueous solution at pH 2.8. A micropattern which had amorphous TiO_2 and octadecyl groups was immersed in an aqueous solution at pH 2.8 for 30 min. Many particles were observed over the whole area of the substrate (Fig. 5), and were formed in the solution homogeneously because of the high degree of supersaturation. These observations are consistent with the results of QCM analysis. XRD measurements for the precipitates deposited for 30 min did not show any peaks since the deposited quantity was not sufficient to show any diffraction. However, the precipitates deposited for 4 h were composed of anatase TiO_2. Anatase TiO_2, which has a large surface area, was deposited from an aqueous solution at low temperature, and may be suitable as a photonic catalyst[5]. However, SSD was not achieved at pH 2.8 because of the deposition of homogeneously nucleated particles, and the control of supersaturation was shown to be important for SSD.

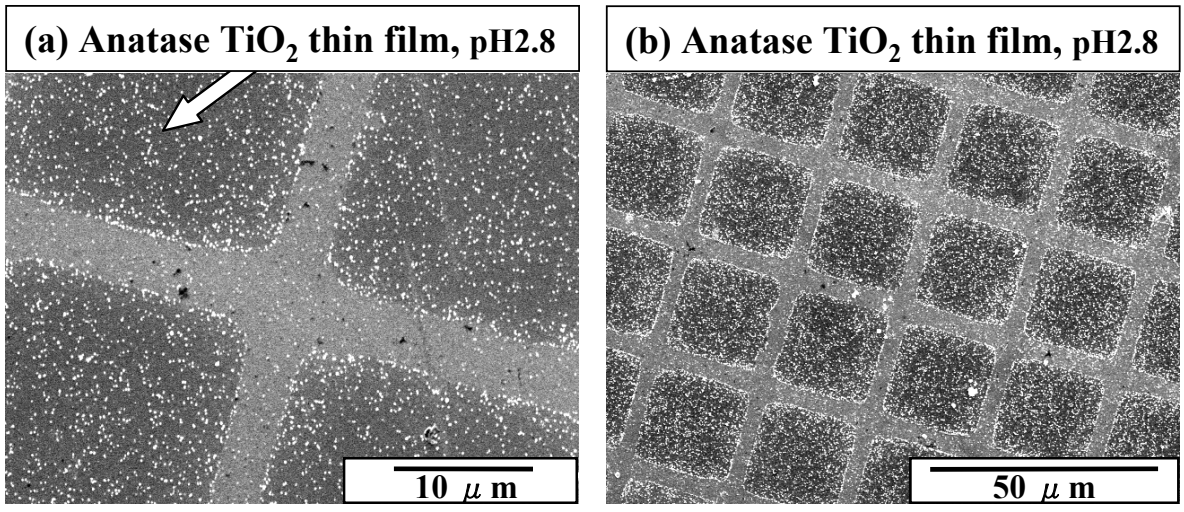

Figure 5. SEM micrographs of a micropattern of anatase TiO_2 thin films deposited at pH 2.8.

Conclusions

We have developed a novel method to realize SSD of thin films using a seed layer. The deposition of anatase TiO_2 from an aqueous solution was shown by QCM analysis to be accelerated on amorphous TiO_2 thin films compared with on octadecyl, phenyl, amino or hydroxyl groups. A micropattern having amorphous TiO_2 regions and octadecyl regions to be used as a template was prepared and immersed in the aqueous solution. Anatase TiO_2 was successfully deposited on amorphous TiO_2 regions, and amorphous TiO_2 thin film was shown to act effectively as a seed layer to accelerate the nucleation and initial growth of anatase TiO_2. Consequently, SSD was achieved and a micropattern of anatase TiO_2 was fabricated in the aqueous solution using a seed layer.

References

(1) Hehre, W. J. Spartan '02 for Windows, Wavefunction, Inc.: Irvine, CA, USA.

(2) Masuda, Y.; Jinbo Y.; Yonezawa T.; Koumoto, K. *Chem. Mater.* **2002,** 14(3), 1236-1241.

(3) Masuda, Y.; Sugiyama, T.; Lin, H.; Seo, W. S.; Koumoto, K. *Thin Solid Films* **2001**, *382*, 153.

(4) Koumoto, K.; Seo, S.; Sugiyama, T.; Seo, W. S.; Dressick, W. J. *Chem. Mater.* **1999**, *11(9)*, 2305.

(5) Kim, K. J.; Benkstein, K. D.; Lagemaat, J.; Frank, A. J. *Chem. Mater.* **2002,** *14*, 1042-1047.

3.4 Site-selective deposition of anatase TiO_2 thin films in an aqueous solution by site-selective immersion method

Site-selective immersion was realized using a SAM having a pattern of hydrophilic and hydrophobic surfaces alike. In the experiment the solution containing Ti precursor contacted the hydrophilic surface, and briefly came in contact with the hydrophobic surface via our new method.

Surfacemodification of HFDTS-SAM and OTS-SAM. OTS-SAM and HFDTS (Heptadecafluoro-1,1,2,2, tetrahydrodecyltrichlorosilane) - SAM were prepared by immersing the Si substrate (P-type Si [100]) into an anhydrous toluene solution containing 1 vol% OTS or HFDTS, respectively, for 5 min under a N_2 atmosphere[1-3]. The substrates with SAMs were baked at 120 °C for 5 min to remove residual solvent and promote chemisorption of the SAM. Molecular structure and surface potential of HFDTS molecule are shown in Figure 1. The calculation was performed at the Hartree-Fock/3-21G(*) level utilizing Spartan program (SPARTAN '02 for Windows, Wavefunction, Inc.)[4]. The geometry of HFDTS molecule was optimized and electrostatic potential was described on isoelectron density plane. Distance between fluorine at the end of the molecule and silicon was calculated to be 1.3 nm and this will be thickness of HFDTS-SAM.

The SAMs on silicon substrates were exposed for 2 h to UV light (184.9 nm) (low-pressure mercury lamp, NL-UV253, Nippon Laser & Electronics Lab.) through a photomask to be used as templates for site-selective deposition. The SAMs were kept 150 mm from the light source in the air. UV-irradiated regions became hydrophilic owing to OH group formation, while the non-irradiated part remained unchanged. Formation of HFDTS-SAM and its modification to OH groups by UV irradiation was verified using the water drop contact angle (θw) (Fig. 1). From this experiment, HFDTS-SAM was converted to OH groups by UV irradiation for 2h.

OTS-SAM has a methyl group at the end of a long methylene chain, HFDTS-SAM has a CF_3 group for the end of a $(CF_2)_7(CH_2)_2$ chain. Initially deposited HFDTS-SAM and OTS-SAM showed water contact angles of 115 ° and 96 °, respectively. UV-irradiated surfaces of SAMs were, however, wetted completely (contact angle < 5 °).

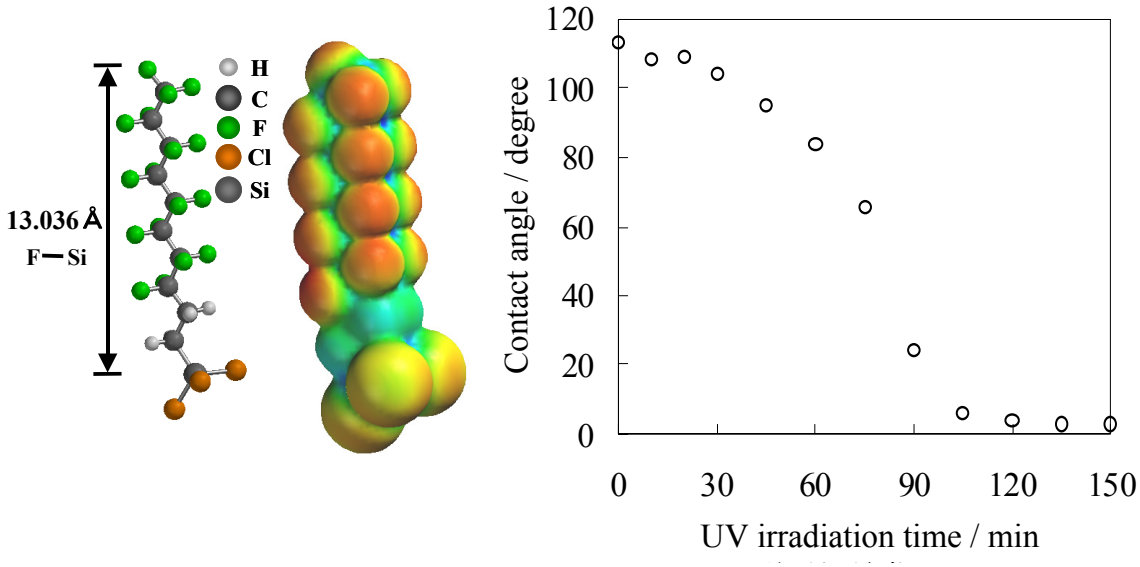

Figure 1. Molecular structure of HFDTS and water drop contact angle for HFDTS-SAM as a function of UV irradiation time.

Fabrication of TiO_2 thin film micropattern by site-selective immersion[5]

HFDTS-SAM or OTS-SAM that have high hydrophobicity were modified by UV irradiation to obtain a pattern of hydrophobic and hydrophilic OH group surfaces (Fig. 2). Patterned SAMs were placed upside down 5 mm above the solution surface. The top clear layer of the solution containing 0.05 M $(NH_4)_2TiF_6$ and 0.15 M (H_3BO_3) kept at pH 2.8 and 50 °C was used for this experiment. Several kinds of solutions were used to form a TiO_2 micropattern, but the top clear layer of the solution was found best for site-selective deposition owing to its supersaturation capability.

Dried air which was desiccated by silica gel and potassium chloride was passed for 4 h through a tube by a pump (Air pump HIBLOW SPP-6EBS, 100V, 8.5 W, Takatsuki Denki Co., Ltd.) 20 mm below the surface of the solution. Bubbles several millimeters in diameter were generated and moved on the surface of a patterned SAM. The solution was repelled and moved quickly on the hydrophobic surface, while the hydrophilic surface was wetted by the solution. The solution remaining on the hydrophilic surface was replaced with a new solution by moving bubbles. Consequently, the hydrophilic surface was continuously wetted with the solution, while the hydrophobic surface was covered with the solution only for a short time. TiO_2 was deposited on the hydrophilic surface from the solution but not on its hydrophobic counterpart. Thus site-selective immersion[5] was attained and the difference in immersion time caused site-selective deposition of TiO_2 thin film.

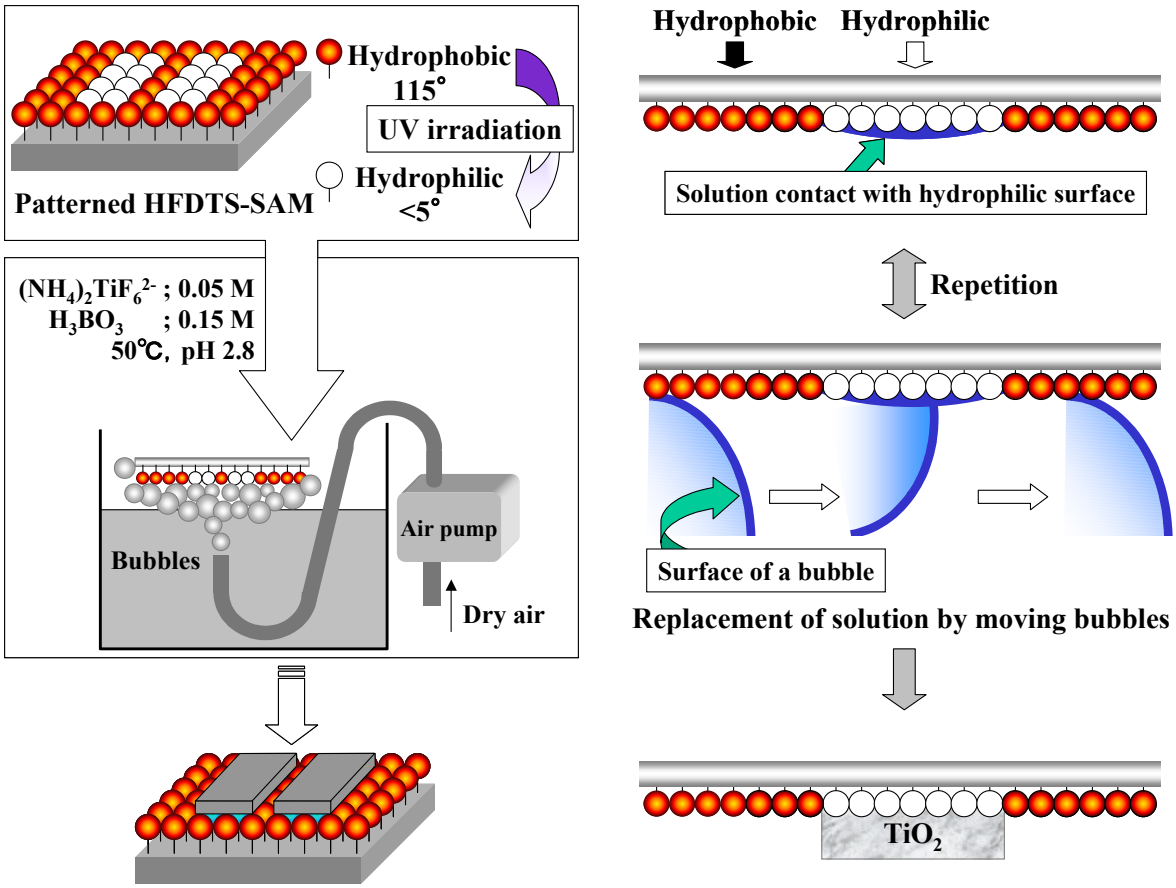

Figure 2. Conceptual process for site-selective immersion to fabricate micropattern of anatase TiO_2 thin film from an aqueous solution.

The feature edge acuity of the micropattern fabricated on a patterned HFDTS-SAM by site-selective immersion (Fig. 3[a]) was estimated from scanning electron microscope (SEM; S-3000N, Hitachi, Ltd.) images to be 11 % and is much better than that of the pattern fabricated via the lift-off process[1] (Fig. 3[b]). The thicknesses of them were 1.3 μm (Fig. 3[a]) and 4.3 μm (Fig. 3[b]), respectively. Furthermore, cracks were not observed in thin films and a smooth surface was obtained (Fig. 3[a]). Deposited films showed an XRD pattern of anatase type TiO_2 and its orientation was similar to that of films deposited in the solution[1] (Fig. 4).

Surface roughness (RMS) was estimated using an atomic force microscope (AFM; Nanoscope E, Digital Instruments) image (Fig. 5) using the equation:

$$\text{RMS (standard deviation)} = [\Sigma_i (Z_i - Z_{ave})^2 / n]^{1/2} \quad \cdots(c)$$

Z_i : height at point "i", Z_{ave} : average of Z (height), n : number of data points

The AFM image shows film roughness to be 43.7 nm, with film thickness near the edge higher than at the interior.

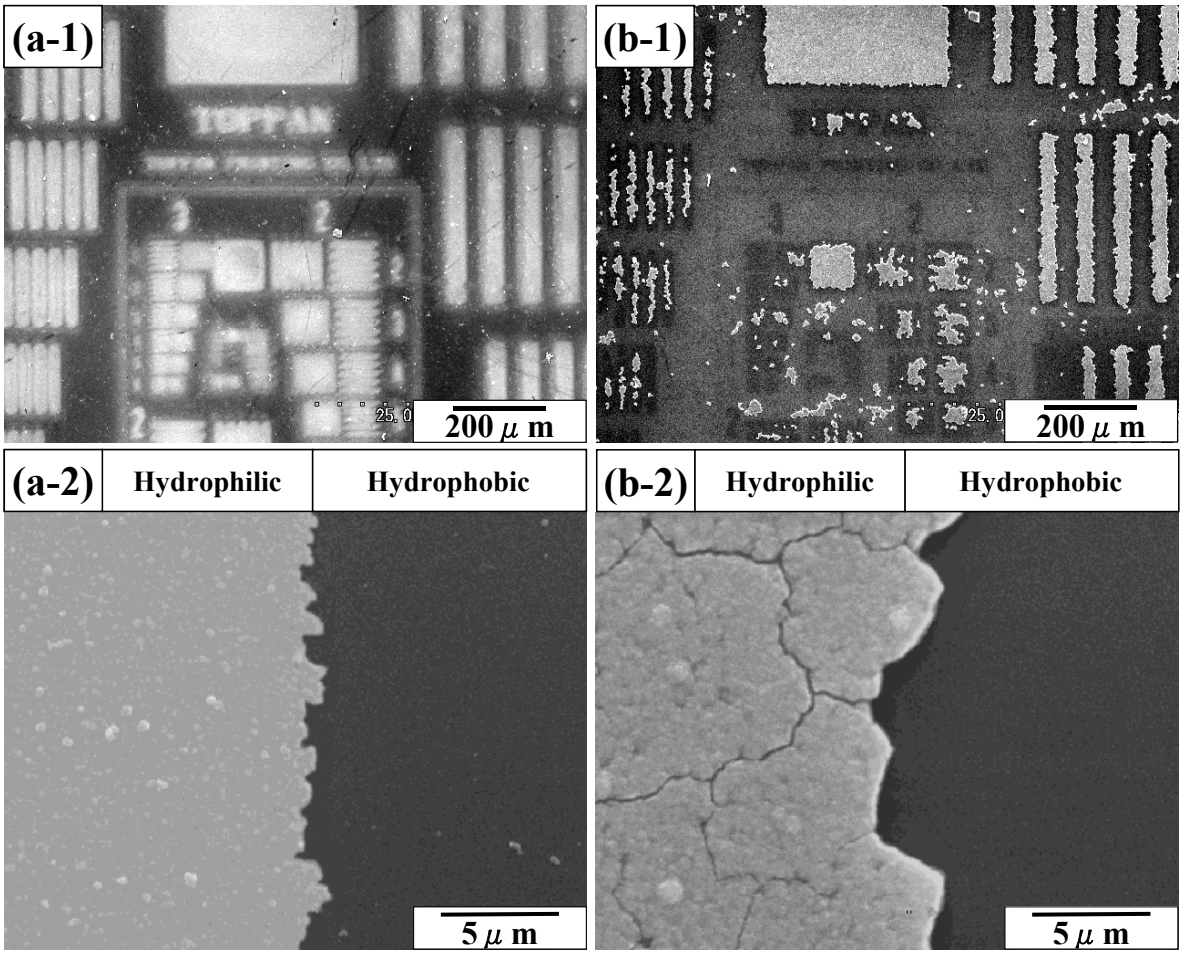

Figure 3. SEM micrographs of micropatterns of TiO_2 thin films on HFDTS / OH-patternd SAM fabricated by (a) site-selective immersion or (b) lift-off process.[1]

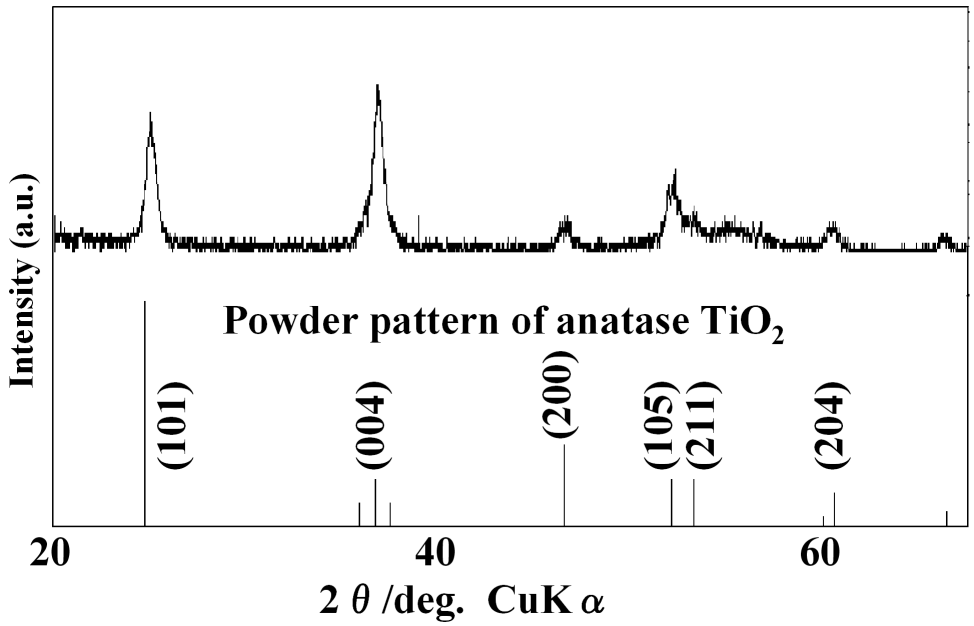

Figure 4. XRD pattern of anatase type TiO_2 deposited on OH groups. Randomly oriented powder pattern for anatase (JCPDS Card No. 21-1272) is shown for comparison.

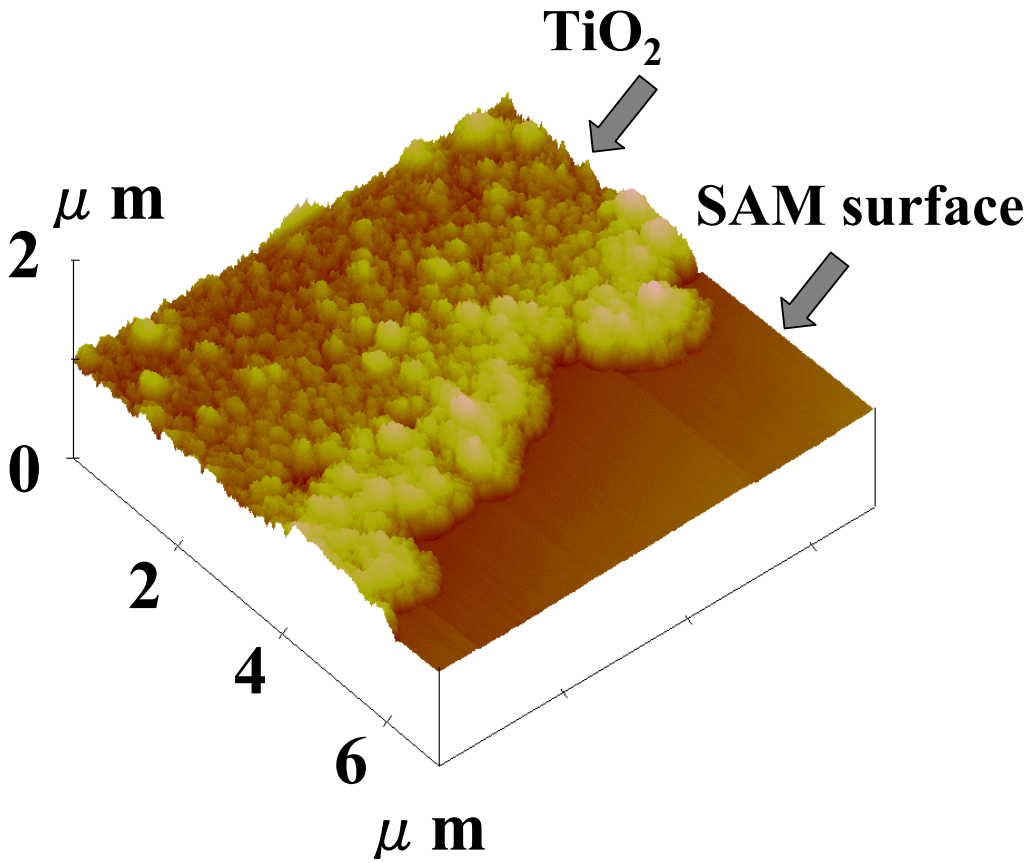

Figure 5. AFM image of micropattern of TiO_2 thin film on HFDTS / OH-patternd SAM fabricated by site-selective immersion.

While a TiO_2 thin film micropattern was also formed on OTS-SAM instead of HFTDS-SAM from the same solution, its feature edge acuity was lower than that of the micropattern generated on patterned HFDTS-SAM. OTS-SAM, which has low hydrophobicity compared with HFDTS-SAM, cannot repel enough solution and suppress TiO_2 deposition. This indicates a pattern possessing a highly hydrophilic surface and that a highly hydrophobic surface would satisfy the requirements for a template to realize site-selective immersion via our method.

Additionally, patterned HFDTS-SAM or OTS-SAM were immersed in the solution containing 0.05 M $(NH_4)_2TiF_6$ and 0.15 M (H_3BO_3) at pH 1.5 or pH 2.8 at 50 °C without the use of site-selective immersion method. TiO_2 thin films were deposited on entire area of patterned SAMs. HFDTS-SAM and OTS-SAM showed a water contact angle of 20 - 50 ° after immersion for 1 h. SAM hydrophobicity decreased by nucleated or adhered TiO_2 particle, and failed to repel enough solution. One probable cause is that pinholes and other defects in the films provides at least some degree of access of water to underlying unreacted OH groups in the HFDTS and OTS films. Once exposed to the solution, these sites can act as nucleation points

for TiO_2 growth. Because the depositions are done at elevated temperatures, it is likely that pinholes and defects will continually open and close on the HFTDS and OTS film surfaces due to thermal motions of alkyl chains in these films. The TiO_2 precursors formed in these defects would contribute to the decreased hydrophobicity and act as points for eventual growth of TiO_2 over the entire SAM-covered region. This would provide a weakly bound TiO_2 film on the HFDTS and OTS film regions due to the limited number of connections to the underlying silanol sites in these film regions. In fact, Sagiv and others have shown that macroscopic defects induced in alkylsiloxane films can readily be accessed by solution species[6-8] More recently, Dressick and coworkers have demonstrated that solvent accessibility to underlying substrates in aromatic siloxane films is also important[4, 9-10] and may even be a greater factor in controlling the properties of those films, an observation which may account for our previous selectivity observation using phenylsiloxane films, as shown in Fig. 3(b).

Patterned HFDTS-SAM or OTS-SAM were placed 5 mm below the surface of the solution, putting both hydrophilic and hydrophobic surfaces in contact with the solution for an extended period of time, and TiO_2 was deposited on both. The feature edge acuity of TiO_2 thin film micropattern (18 %) was lower than that of the micropattern formed on a patterned SAM kept above the solution.

The micropattern of TiO_2 thin film was also formed using air more humid than the dried air. However, the thin film pattern feature edge acuity (13 %) was slightly lower than that made using dry air. Though it was bubbled through water and took up water molecules from the solution, dried air was passed only 20 mm and the humidity in dried air bubbles would be lower than that of air. A part of water molecules in air probably contact to HFDTS-SAM and this decrease hydrophobicity of the SAM. This makes contact time of solution to HFTDS-SAM slightly longer and induces growth of TiO_2. Higher humidity in bubbles of air may induce the solution to contact the hydrophobic surface so that the amount of TiO_2 deposited on the surface increases by the use of air.

These experiments show the site-selective immersion method as sensitive to the conditions of solution and substrates surface. In particular, surface supersaturation and hydrophobicity should be well controlled to realize site-selective immersion for fabricating the micropattern of TiO_2 thin films. Since HFDTS-SAM repels not only a water solution but also an organic solvent such as toluene, the site-selective immersion method we developed can be applied to fabricating micropatterns of any kind so long as the film can be deposited from a solution.

Conclusions

Site-selective immersion was achieved using air bubbles which move continuously on the substrate with a hydrophilic/hydrophobic patterned surface. A micropattern of anatase type TiO_2 thin film having no cracks and high feature edge acuity was successfully fabricated by the site-selective immersion method.

References

(1) K. Koumoto, S. Seo, T. Sugiyama, W. S. Seo, W. J. Dressick, *Chem. Mater.,* **1999**, *11(9)*, 2305.

(2) Y. Masuda, T. Sugiyama, H. Lin, W. S. Seo, K. Koumoto, *Thin Solid Films,* **2001**, *382*, 153.

(3) Y. Masuda, M. Itoh, T. Yonezawa, K. Koumoto, *Langmuir,* **2002**, *18 (10)*, 4155 –4159.

(4) W. J. Dressick, P. F. Nealey, S. L.Brandow, *Proc. SPIE,* **2001**, *4343*, 294-305.

(5) Japanese Patent Application Serial Number 2002-137641

(6) J. Gun and J. Sagiv, *J. Colloid Interface Science,* **1986**, *112*, 457-472.

(7) M. E. McGovern, K. M. R. Kallury, M. Thompson, *Langmuir,* **1994**, *10*, 3607-3614.

(8) J. Duchet, B. Chabert, J. P.Chapel, J. F. Gerard, J. M. Chovelon, N. Jaffrezic-Renault, *Langmuir,* **1997**, *13*, 2271-2278.

(9) W. J. Dressick, M-S. Chen, S. L. Brandow, *J. Amer. Chem. Soc*., **2000**, *122*, 982-983.

(10) W. J. Dressick, M-S. Chen, S. L. Brandow, K. W. Rhee, L. M. Shirey, F. K. Perkins, *Appl. Phys. Lett.,* **2001**, *78*, 676-678.

3.5 Site-selective deposition of anatase TiO_2 thin films in an aqueous solution by site-selective elimination method

In this study we developed a novel method to realize site-selective deposition of thin films using a site-selective elimination method. The concept of this method is the use of the difference in adhesion strength of the depositions to the substrate.

Site-selective elimination and nano/micro-scaled pattern of thin films. After having been immersed in the solution with ultrasonic treatment (Fig. 1), the substrates were rinsed with distilled water and observed by an optical microscope (BX51WI with CCD camera), an optical microscope (BX51WI Microscope, Olympus Optical Co., Ltd.) with a digital camera (DP50, 5.8 megapixels, Olympus Optical Co., Ltd.) and a computer for capturing data, a scanning electron microscope (SEM; S-3000N, Hitachi, Ltd.), and a scanning probe microscope (SPI 3800N, Seiko Instruments Inc.) that was operated in AFM (atomic force microscopy) tap mode to observe the topography of the surface. AFM scans were operated at room temperature under ambient air. We used an old SAM for Fig. 2 (b) to check the influence of pinholes and defects in the SAM for TiO_2 deposition. An SAM was kept in air for 1 month after preparation and was patterned by UV irradiation. The patterned SAM, which probably had many pinholes and other defects, was then immersed in the solution to deposit TiO_2 thin films. Thin films were observed on the silanol group regions to form nano/micro-scaled patterns at pH 3.88, 2.8 or 1.5. The films deposited for 4 h from the solution without the addition of HCl are shown in Figs. 2–4. Thin films were observed as being dark in an optical micrograph (Fig. 2) and the reflection of incident radiation by thin films was observed particularly in the upper right region. Separated parallel lines 200–400 nm in width at 100–200 nm intervals were successfully fabricated with this method (Fig. 2 (a-b)). The length of the separated parallel lines reached more than 100 μm (Fig. 2 (a-b)). A cross section of the lines was shown as a semicircle, and the thickness of the center of the lines was estimated to be about 100 nm by AFM observation (Fig. 3). Feature edge acuity of the pattern was higher than that of the pattern fabricated by our lift-off process[1] or by the site-selective immersion method.[2-3]

Depositions on octadecyl group regions were peeled off mechanically by ultrasonication during immersion because depositions have weak adhesion strength to octadecyl groups compared with depositions on silanol groups.[1] On the other hand, depositions on silanol group regions were retained and thin films were thus formed on silanol group regions selectively. The

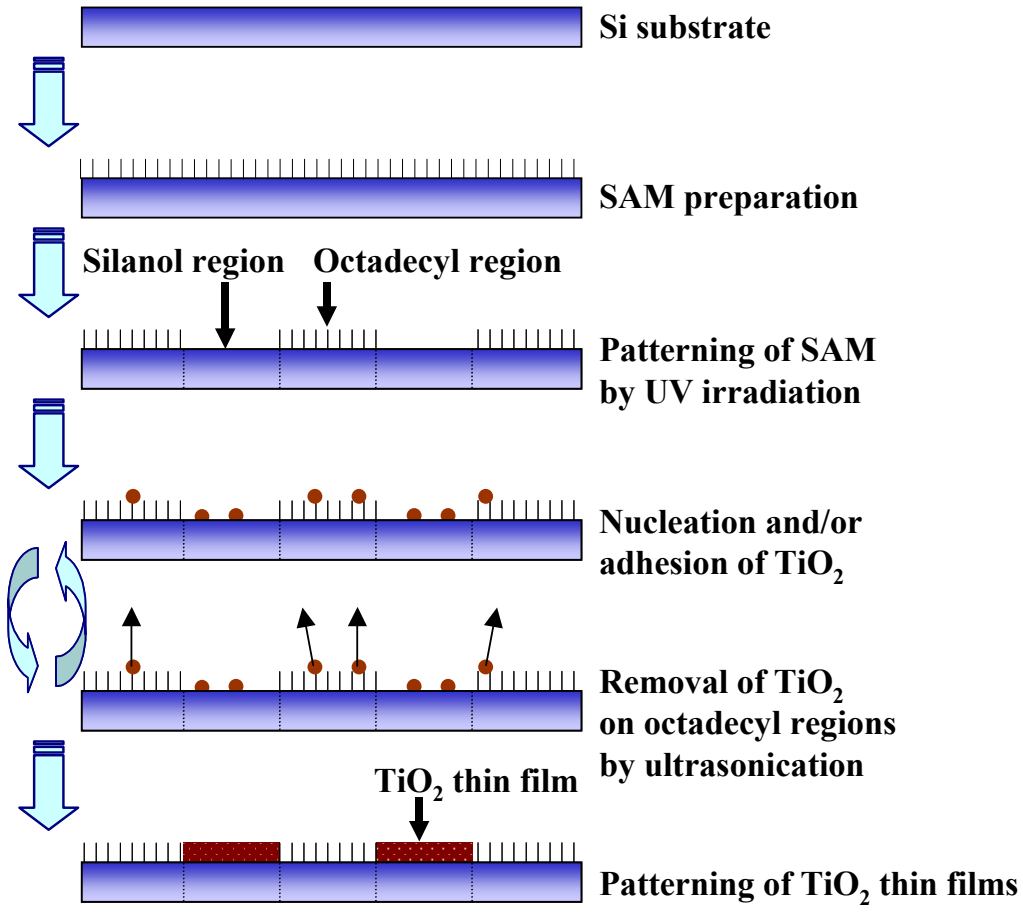

Figure 1. Conceptual process of site-selective elimination for the patterning of anatase TiO_2 thin films from an aqueous solution.

difference in adhesion strength of the depositions to substrate allowed us to realize site-selective elimination and the fabrication of nano/micr o-scaled patterns in the solution. This difference is presumably caused by the difference in chemical bonds between depositions and substrates. Titanium precursors can form chemical bonds such as Si-O-Ti with silanol groups and have strong adhesion to the surface of silanol groups, whereas octadecyl groups cannot form chemical bonds with Ti precursors. However, some depositions were observed on octadecyl group regions in Fig. 2 (b). One probable cause is that pinholes and other defects in the films provide at least some degree of access of water to underlying unreacted OH groups in the OTS films. Once exposed to the solution, these sites can act as nucleation points for TiO_2 growth. Because the depositions are performed at elevated temperatures, it is likely that pinholes and defects will continually open and close on the OTS film surfaces due to thermal

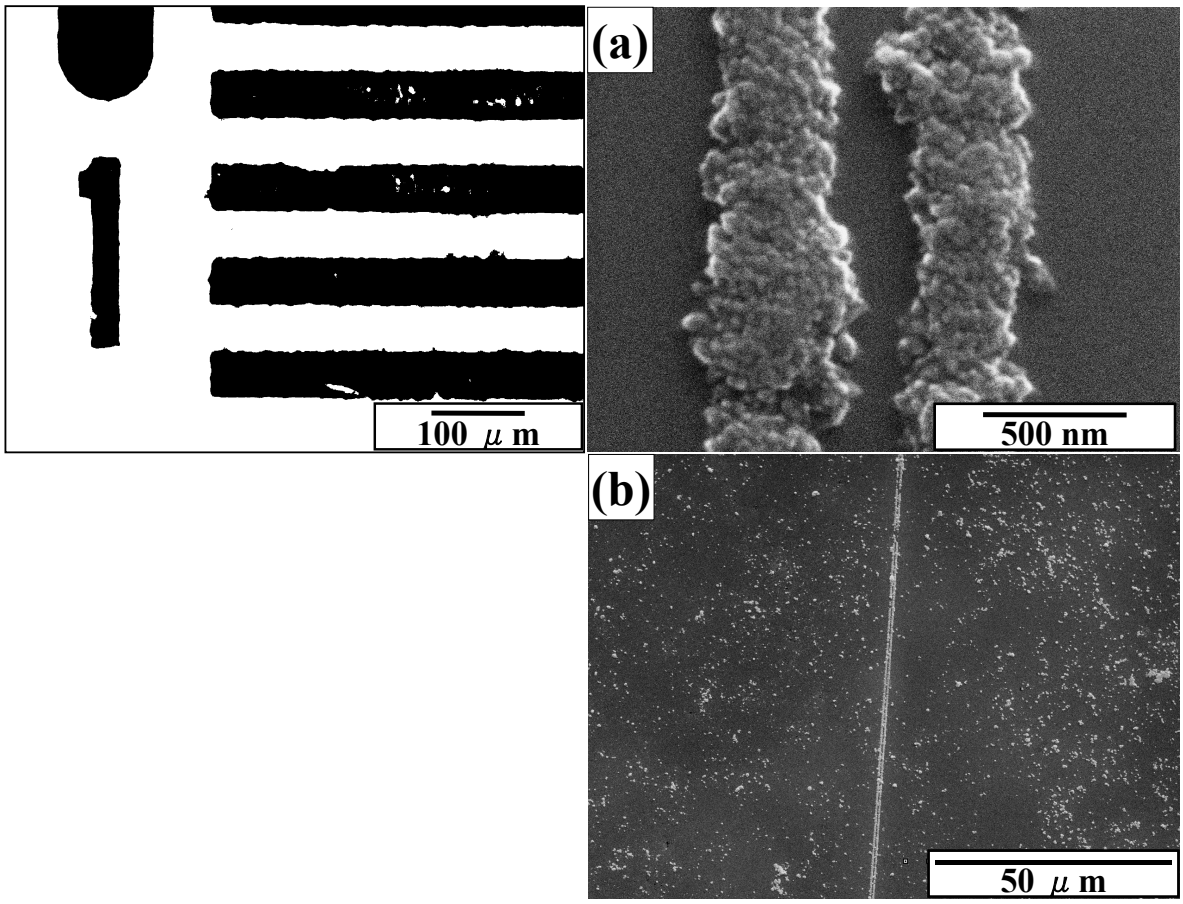

Figure 2. Optical micrograph and (a), (b) SEM micrographs of micropattern of anatase TiO_2 thin films.

motions of alkyl chains in the films. The TiO_2 precursors formed in these defects would act as points for eventual growth of TiO_2 over the entire SAM-covered region. This would provide a weakly bound TiO_2 film on the OTS film regions due to the limited number of connections to the underlying silanol sites in the film regions. In fact, Sagiv and others have shown that macroscopic defects induced in alkylsiloxane films can readily be accessed by solution species.[4-6] More recently, Dressick and coworkers demonstrated that solvent accessibility to underlying substrates in aromatic siloxane films is also important[7-9] and may be an even greater factor in controlling the properties of those films, which may account for our previous selectivity observation using phenylsiloxane films, as shown in the lift-off process.[1]

In the lift-off process,[1] thin films were formed on the entire area of patterned SAM that has silanol group regions and phenyl (or octadecyl) group regions. After being dried, the substrate was sonicated in water to lift off thin films on phenyl (or octadecyl) group regions selectively. Thin films on phenyl (or octadecyl) group regions were peeled off along the cracks that formed

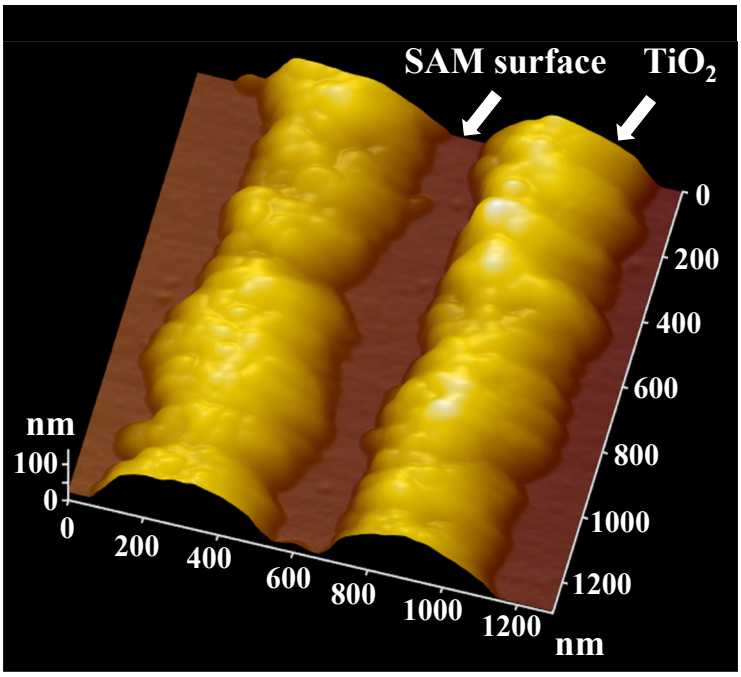

Figure 3. AFM image of micropattern of anatase TiO_2 thin films on OTS/OH-patterned SAM fabricated by LPD using ultrasonication.

during the drying process. Thin films on phenyl (or octadecyl) group regions without cracks were not peeled off because depositions strongly connected to each other to form solid timber (monolith). The lift-off along cracks decreased the feature edge acuity of the pattern in this method. Thin films were formed on silanol group regions selectively and site-selective deposition was realized with our newly developed method. This resulted in high feature edge acuity of the patterns compared to our previous works.[1]

Additionally, the micropattern of thin films was also fabricated by the site-selective immersion method. A solution containing a Ti precursor contacted the hydrophilic regions during the experiment and briefly came into contact with the hydrophobic regions. The solution on the hydrophilic surface was replaced with a fresh solution by continuous movement of bubbles. Thus TiO_2 was deposited and a thin film was grown on the hydrophilic regions selectively. This technique can be applied for the formation of many kinds of films from any solution and to fabricate micropatterns for many kinds of thin film because the technique creates the difference in contact time of the solution between hydrophilic regions and hydrophobic regions. However, it is difficult to form a solution layer on nano-scaled hydrophilic regions selectively and replace it with a fresh solution by continuous movement of bubbles while avoiding contact of the solution on hydrophobic regions. This prevents

fabrication of nano-scaled pattern with this method. On the other hand, site-selective deposition was realized in the solution with our newly developed method using the difference of adhesion strength of depositions to substrates. Heterogeneously nucleated deposition and homogeneously nucleated particles and/or clusters can be removed from octadecyl group regions even if these regions are designed in nano-scale order in which depositions are smaller. This allowed us to realize high feature edge acuity of the patterns compared to site-selective immersion.[2-3, 10]

Characterizations of thin films. The distribution of elements on the surface of the substrates was evaluated by energy dispersive X-ray analysis (EDX; EDAX Falcon, EDAX Co. Ltd.), which is built into SEM. Titanium was detected from thin films selectively and oxygen was detected mainly from silanol group regions by EDX (Fig. 4). Other elements, except for silicon from a substrate, were not observed from the thin film and substrate by EDX. Oxygen was detected from not only the deposited thin film but also from the natural oxide layer (amorphous SiO_2 layer) formed on all surface areas of a silicon substrate. These observations showed predominant deposition of titanium oxide on silanol group regions.

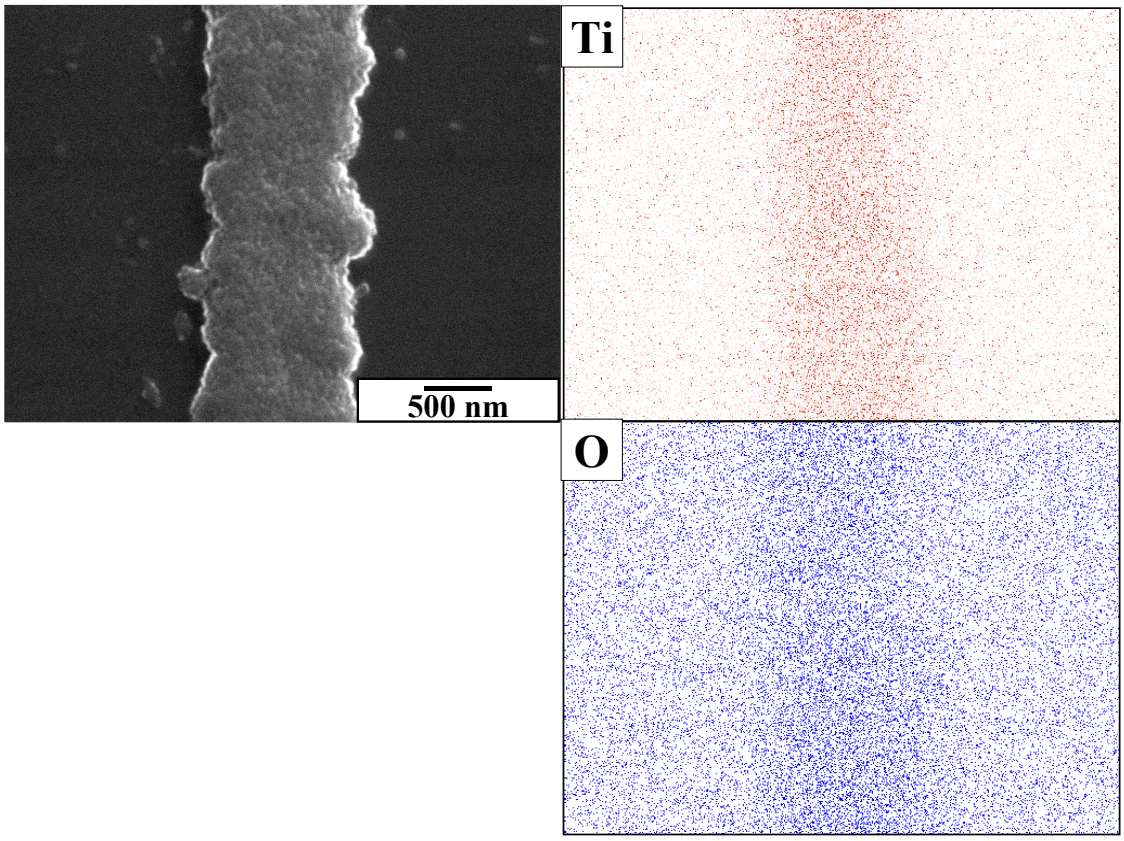

Figure 4. SEM micrograph of micropattern of anatase TiO_2 thin film (a) and EDX images for Ti and O.

The deposited thin films were also investigated using an X-ray diffractometer (XRD; RAD-C, Rigaku) with CuKα radiation (40 kV, 30 mA) and Ni filter plus a graphite monochromater. Thin films deposited at pH 3.8 for 4 h showed an XRD pattern of anatase-type TiO_2 having orientation similar to that of films deposited in the solution at pH 1.5 or 2.8[1-3] (Fig. 5). The diffraction from parallel to c-plane such as (004) was observed as being strong compared to that of the randomly oriented powder diffraction pattern (Fig. 5). The orientation and crystal growth mechanism are discussed in a separate article.[11]

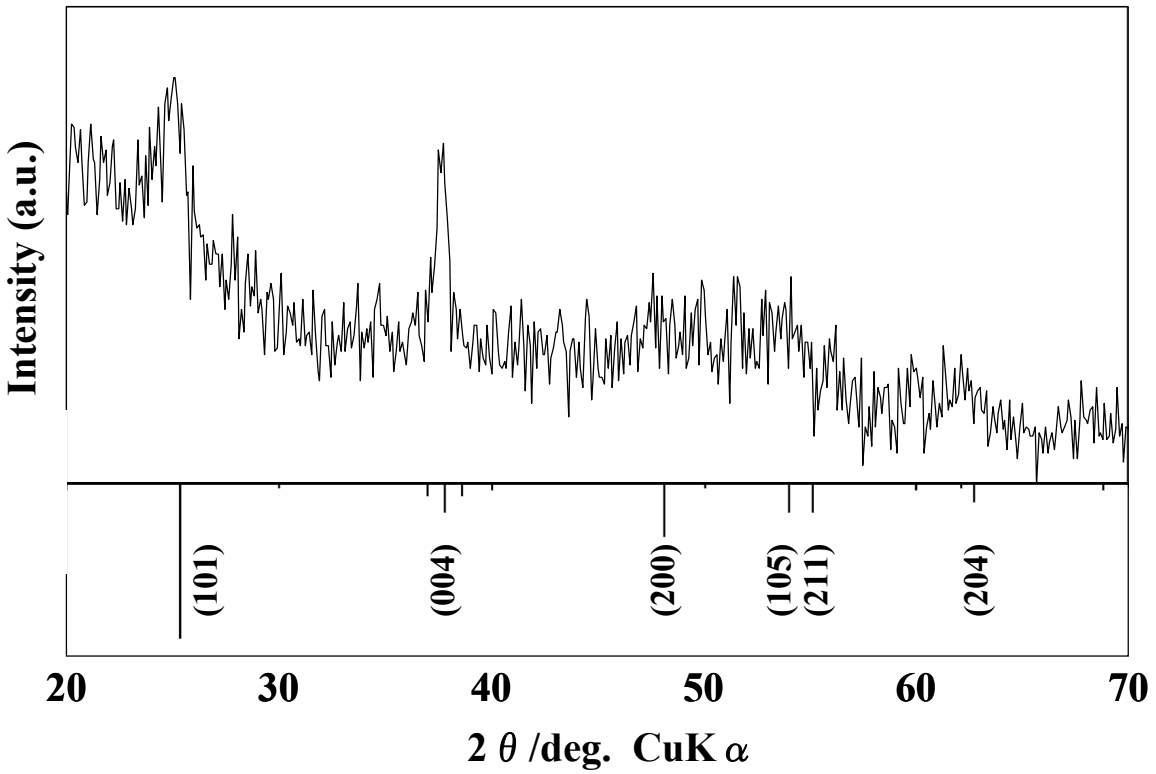

Figure 5. XRD pattern of deposited thin films on silanol group regions from an aqueous solution.

Thin films were further evaluated by X-ray photoelectron spectroscopy (XPS; ESCA-3200, Shimazu Corporation, 1×10^{-5} Pa). The X-ray source (MgKα, 1253.6 eV) was operated at 8 kV and 30 mA. The spectral peaks corresponding to Ti 2p (458.7 eV) were observed from thin films deposited on the silanol region (Fig. 6). This binding energy is higher than that of Ti metal (454.0 eV), TiC (454.6 eV), TiO (455.0 eV), TiN (455.7 eV) and Ti_2O_3 (456.7 eV), and similar to that of TiO_2 (458.4 - 458.7 eV).[12-14] This suggests that the titanium atoms in thin films are positively charged relative to that of titanium metal by formation of direct bonds with

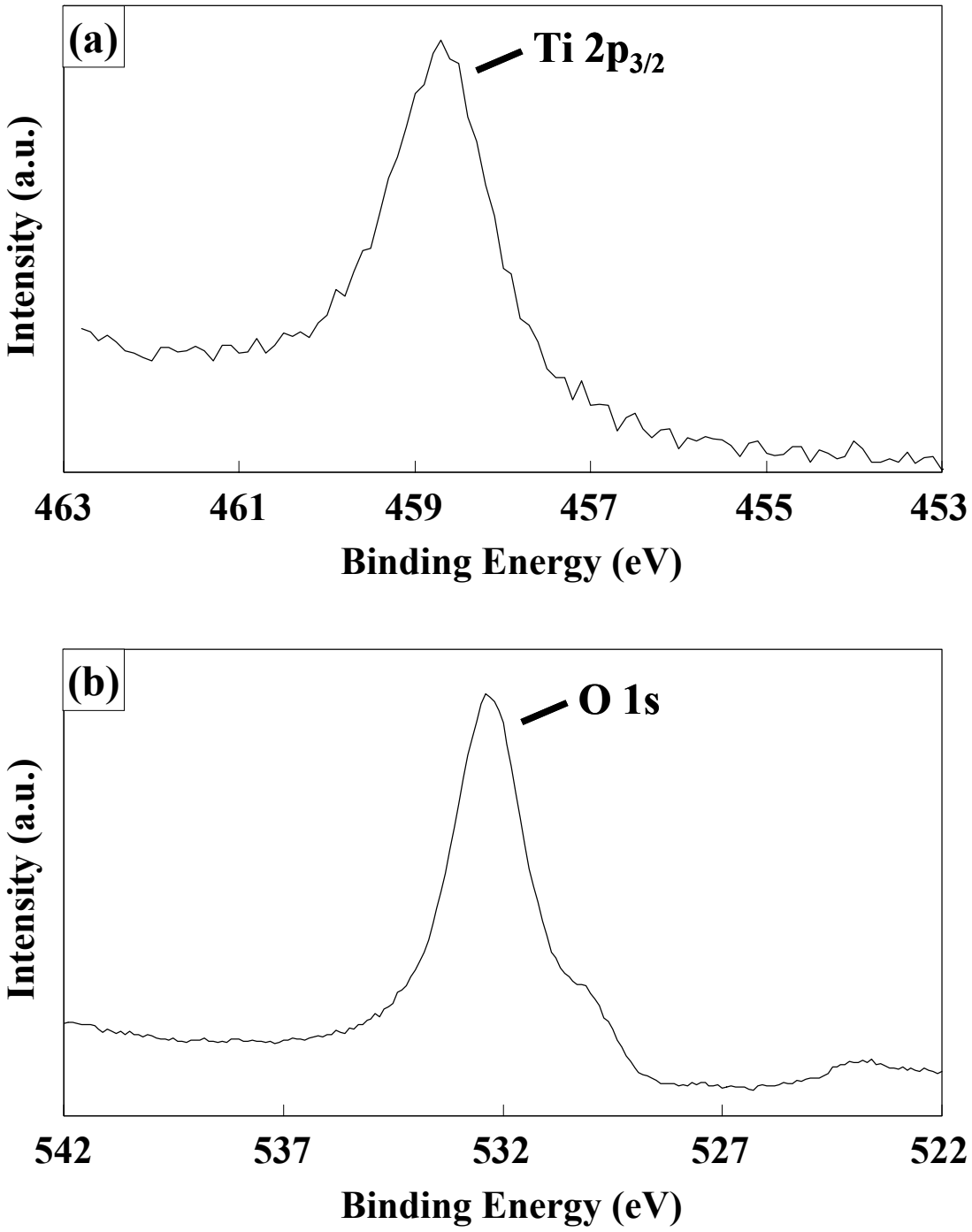

Figure 6. XPS spectra of (a) Ti 2p and (b) O 1s for deposited thin films from an aqueous solution.

oxygen. On the other hand, this spectrum was not observed from octadecyl group regions. The O 1s spectrum was observed from the silanol regions and divided into O 1s (530.2 eV) and O 1s (532.3 eV). O 1s (532.3 eV) can be assigned to the silicon oxide layer on the surface of the

silicon wafer (532.0 eV[13]). The binding energy of O 1s (530.2 eV) is similar to that of TiO_2 (529.9 eV[14], 530.1 eV[13]), and shows that oxygen is negatively charged compared with neutral oxygen molecules (531.0 eV), possibly through the formation of chemical bonds with Ti. The ratio of titanium to oxygen was estimated from the Ti $2p_{3/2}$ (458.7 eV) spectrum and O 1s (530.2 eV) spectrum to be Ti:O = 1:2.0.

Conclusions

We proposed a novel method to fabricate nano/micro-scaled patterns of thin films and successfully fabricated patterns of anatase TiO_2 thin films in an aqueous solution at 50 °C. The difference in adhesion strength of thin films on substrates was employed for the site-selective elimination method. Heterogeneously nucleated TiO_2 and adhered homogeneously nucleated TiO_2 particles on OTS-SAM can be easily eliminated from the substrate by ultrasonication, whereas those on silanol groups maintained their adhesion during the immersion period. The essence of the site-selectivity of this method is a difference in adhesion strength. The site-selective elimination method can be applied to fabricate nano/micro-scaled patterns in the solution by the immersion of the substrate that has regions on which depositions adhere strongly and regions on which depositions adhere weakly enabling elimination by treatment such as ultrasonication.

References

(1) Koumoto, K., Seo, S., Sugiyama, T., Seo, W.S. and Dressick, W.J. *J. Chem. Mater.* **1999**, *11(9)*, 2305.

(2) Masuda, Y., Sugiyama, T. and Koumoto, K. *J. Mater. Chem.* **2002**, *12(9)*, 2643-2647.

(3) Japanese Patent Application Serial Number 2002-137641.

(4) Gun, J. and Sagiv, J. *J. Colloid Interface Science,* **1986**, *112*, 457-472.

(5) McGovern, M.E., Kallury, K.M.R. and Thompson, M. *Langmuir,* **1994**, *10*, 3607-3614.

(6) Duchet, J., Chabert, B., Chapel, J.P., Gerard, J.F., Chovelon, J.M. and Jaffrezic-Renault, N. *Langmuir,* **1997**, *13*, 2271-2278.

(7) Dressick, W.J., Chen, M.-S. and Brandow, S.L. *J. Amer. Chem. Soc*., **2000**, *122*, 982-983.

(8) Dressick, W.J., Chen, M.-S., Brandow, S.L., Rhee, K.W., Shirey, L.M. and Perkins, F.K. *Appl. Phys. Lett.,* **2001**, *78*, 676-678.

(9) Dressick, W.J., Nealey, P.F. and Brandow, S.L. *Proc. SPIE,* **2001**, *4343*, 294-305.

(10) Masuda, Y., Ieda, S. and Koumoto, K. *Langmuir,* **2003**, *19(10)*, 4415-4419.

(11) Masuda, Y., Sugiyama, T., Seo, W.S. and Koumoto, K. *Chem. Mater.,* submitted.

(12) Masuda, Y., Sugiyama, T., Lin, H., Seo, W.S. and Koumoto, K. *Thin Solid Films* **2001**, *382*, 153.

(13) Huang, D., Xiao, Z.-D., Gu, J.-H., Huang, N.-P. and Yuan, C.W. Thin Solid Films 305 (1997) 110-115.

(14) Zhang, F., Jin, S., Mao, Y., Zheng, Z., Chen, Y. and Liu, X. Thin Solid Films 310 (1997) 29.

3.6 Deposition mechanism of anatase TiO_2 on self-assembled monolayers from an aqueous solution

We evaluated in detail the deposition process of anatase TiO_2 from an aqueous solution.

Zeta potential of TiO_2 particles. In the solution at pH 2.8, many homogeneously nucleated particles were deposited on the substrate and grew to form thin films because of the solution's high degree of supersaturation (Fig. 1). It is important to understand the interactions between homogeneously nucleated particles and a substrate in order to investigate the deposition mechanism. Therefore, we evaluated the zeta potential of homogeneously nucleated TiO_2 particles in the solution.

TiF_6^{2-} 0.05 M solution and BO_3^{3-} 0.015 M solution were kept at 50 °C for 24 h. They were then mixed and kept at 50 °C for 30 min to grow TiO_2 particles. The surface character (zeta potential) of homogeneously nucleated anatase TiO_2 particles in the solution containing TiF_6^{2-} ions and BO_3^{3-} ions was examined by direct measurement of electrophoretic mobility using an electrophoretic light scattering spectrometer (Zetasizer 3000HS, Malvern Instruments Co., Ltd.). The zeta potential of TiO_2 particles was determined to be –14 mV at pH 2.8 (Fig. 2), though the isoelectric point (IEP) of TiO_2 was reported to be 2.7–6.0 (anatase)[1], 3.4–5.5 (rutile)[1], 5.6 (rutile)[2], 5.9 (rutile)[3], or 6.2 (rutile).[4] The zeta potential of anatase TiO_2 particles in the solution was also confirmed to be negative in these pH regions (–16.6 V at pH 3.8 (plotted in Fig. 2)) with another electrophoretic light scattering spectrophotometer (ELS-8000, Otsuka Electronics Co., Ltd.).

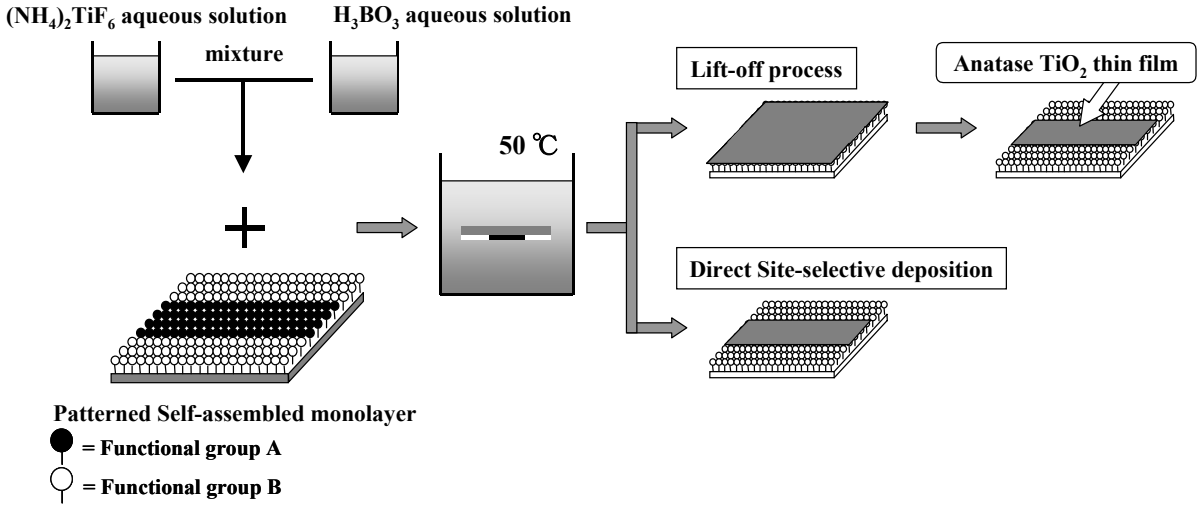

Figure 1. Conceptual process for fabricating a micropattern of anatase TiO_2 thin film from an aqueous solution.

Zeta potential is very sensitive to the surface conditions of particles, ions adsorbed on the particle surfaces, and the kinds and concentrations of ions in the solution. The variations in zeta potential were likely caused by the difference in the surface conditions of TiO_2 particles affected by the interactions between particles and ions in the solution.

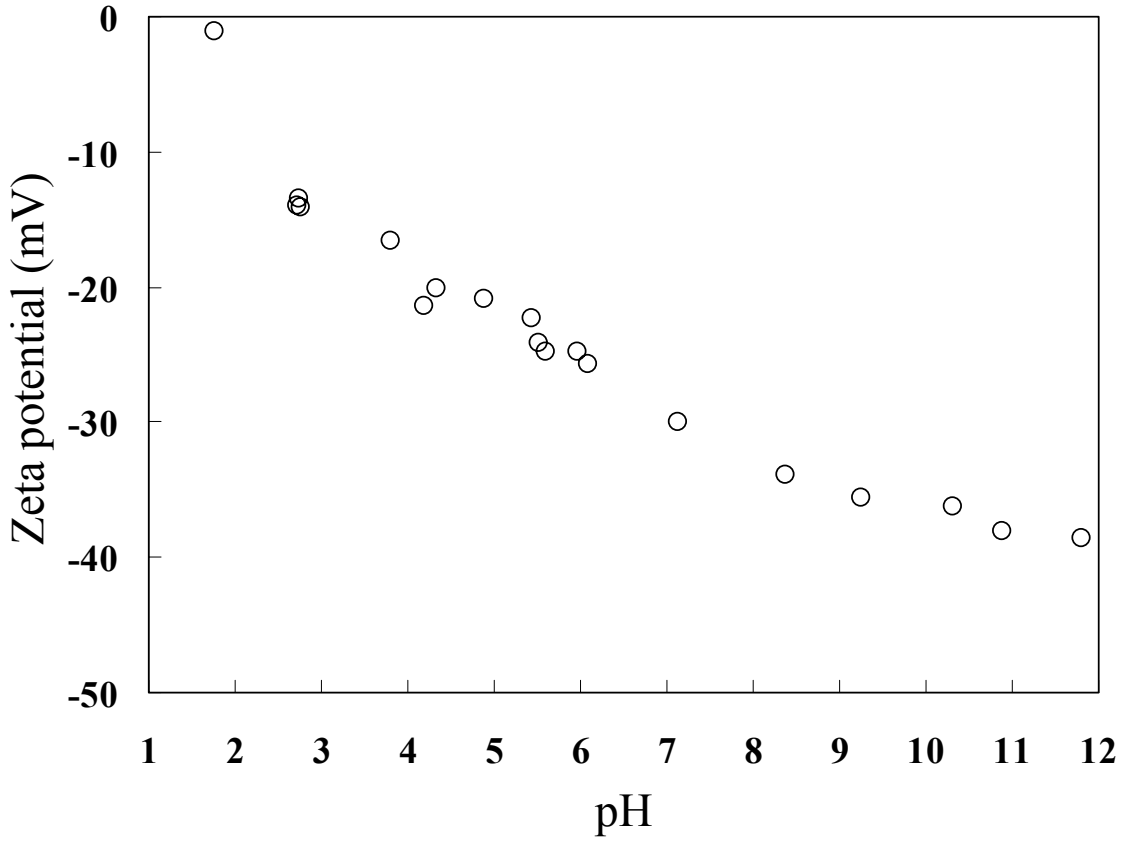

Figure 2. Zeta potential of homogeneously nucleated TiO_2 particles in the solution containing TiF_6^{2-} and BO_3^{3-} ions.

The adsorption of ions which affect zeta potential was observed in HCl[5], KCl[5], $BaCl_2$[5], KOH[5], dodecyl trimethylammonium bromide (DATB)[6] and sodium dodecyl sulfate (SDS)[6] aqueous solutions. The zeta potential of rutile in pure water was –17 mV (IEP pH 4.5) and decreased with the addition of sodium dodecyl sulfate (SDS) to –43 mV (SDS: 1 mM).[6] It is concluded that DS^- ions ($C_{12}H_{25}OSO_3^-$) replaced hydroxyl ions (HO^-) on the surface of rutile to decrease zeta potential. The effect of anions should be more pronounced than that of cations under the conditions in our study.

Additionally, the zeta potential of rutile treated at 1000 °C was –18 mV in pure water and decreased with the addition of sodium triphosphate to –53 mV (4×10^4 eq./l).[5] The positively charged surfaces in water were all inverted by the addition of triphosphate, and the negatively charged rutile surface became more

negative, even at an extremely low concentration of triphosphate. This was obviously caused by the strong adsorption of triphosphate, suggesting the formation of a complex compound on the surface of TiO_2.[5] These findings reported in the literature strongly support our conjecture that anions must have adsorbed to the surfaces of TiO_2 particles, giving rise to highly negative zeta potential, as many kinds of anions, such as F^-, BO_3^{3-}, BF_4^- and TiF_6^{2-}, were contained in our solution with the concentration of more than 2×10^{-2} M[4].

We have reported that negatively charged microparticles of hydroxyapatite were drawn to attach to a positive silicon surface covered by amino groups owing to attractive electrostatic force, whereas no particles were observed on a negatively charged silicon surface covered by OH groups.[7] We therefore evaluated deposition rates for several kinds of SAMs at pH 2.8.

Nucleation and crystal growth of TiO_2 on SAMs. SAMs of OM-SAM, PM-SAM, AET-SAM and UV irradiated OM-SAM (OH-SAM) were immersed in the solution containing TiF_6^{2-} 0.05 M and BO_3^{3-} 0.015 M at pH 1.5 (Fig. 3a) and pH 2.8 (Fig. 3b) to evaluate the reaction rate on SAMs in the solution. The degree of supersaturation is high at pH 2.8 since low H^+ concentration promotes TiO_2 generation as indicated by equation (a). Thus, many homogeneously nucleated TiO_2 particles were observed in the solution. Although no significant variation in induction time was observed among these SAMs, the deposition rate on AET(NH_2)-SAM was much higher than that on OH-SAM (OH groups) and showed the following order: APTS(AET)-SAM > OTS(OM)-SAM > PTCS(PM)-SAM > OH-SAM (Fig. 3a). This order of deposition rate is similar to that of zeta potential of SAMs, indicating that negatively charged TiO_2 particles are definitely attracted to positively charged SAMs by the attractive electrostatic interaction and form a TiO_2 film. Accordingly, the amount of TiO_2 deposited on OH-SAM was less than that on APTS(AET)-SAM.

On the other hand, no significant variation in the amount of deposition and deposition rates was observed among the four SAMs at pH 1.5 (Fig. 3b). The solution was transparent during the whole experiment. The supersaturation degree of the solution at pH 1.5 was low due to the high concentration of H^+ which suppressed the deposition of TiO_2. TiO_2 is probably would be deposited mainly by heterogeneous nucleation in this solution, and nucleation and growth events are scarcely affected by surface functional groups of SAMs. This suggests the critical free energy for heterogeneous nucleation of anatase TiO_2 may be similar for the SAMs employed here. Additionally, TiO_2 probably grew on pinholes and other defects in SAMs as reported[8-13] because they can act as nucleation sites for TiO_2 growth. As the deposition was carried out at elevated temperature (50 °C), it is likely that pinholes and defects continuously opened and closed on SAM surfaces due to the thermal motions of organic groups in these films.

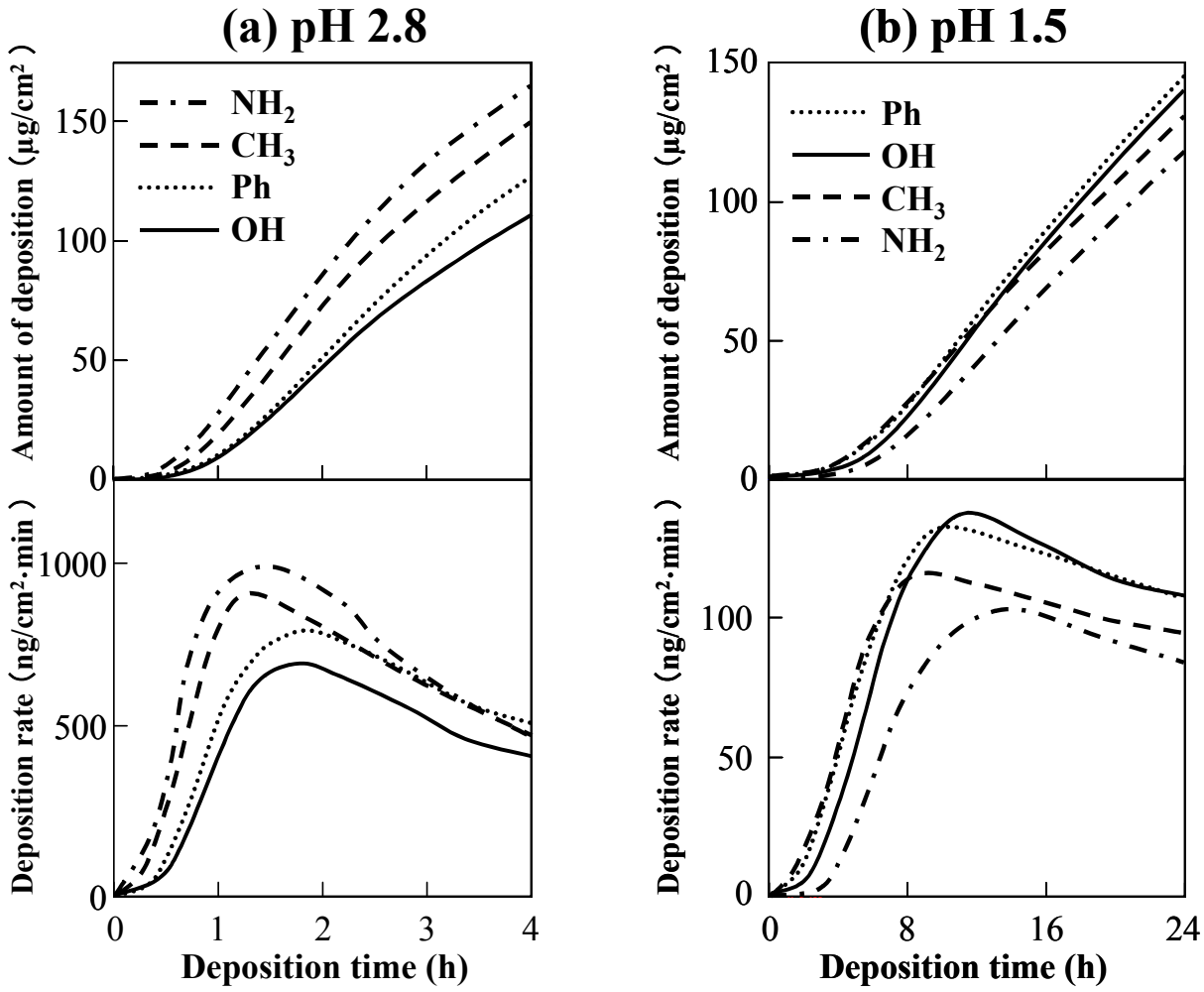

Figure 3. Deposition rate and deposition quantity of TiO_2 in the solution at (a) pH 2.8 or (b) pH 1.5 as a function of deposition time.

Moreover, the numerical density of particles and particle size were measured directly from SEM micrographs (SEM; S-3000N, Hitachi, Ltd.) (Fig. 4). The particle size on the OH-group surface nearly equaled that on other SAMs, although the particle size on OTS-SAM was slightly smaller than that on the OH-group surface at pH 1.5. Whereas the particle size on each SAM increased with reaction time (240 nm (6 h), 380 nm (12 h), 530 nm (18 h), 1100 nm (24 h) at pH 1.5, and 400 nm (1 h), 480 nm (2 h), 770 nm (3 h), 960 nm (4 h) at pH 2.8), the numerical density of particles reached a maximum after 10–16 h of reaction at pH 1.5 or after 1–2 h of reaction at pH 2.8 (Fig. 5). This shows that small particles were incorporated into large particles since they began to contact each other after these periods. The difference in amount of deposition determined from QCM measurements did not stem from particle size variations but from particle density. The order of particle numerical density at pH 2.8 (NH_2 > CH_3 > Ph > OH) (Fig. 5b) agrees with the order of the amount of deposition at pH 2.8 measured by QCM (Fig. 3b).

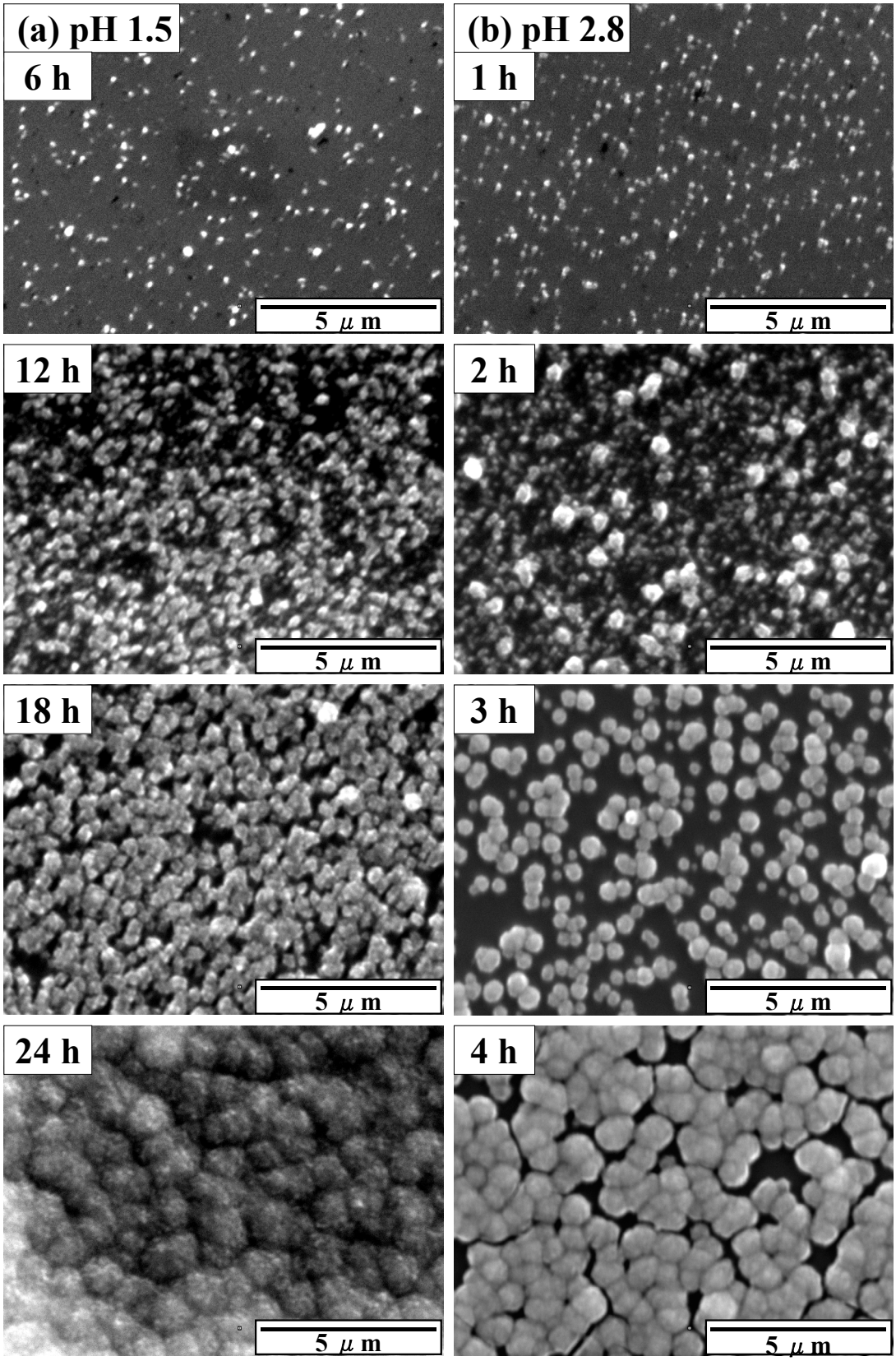

Figure 4. SEM micrographs of (a) TiO_2 on OH groups deposited for 6, 12, 18 or 24 h in the solution at pH 1.5 and (b) TiO_2 on OH groups deposited for 1, 2, 3 or 4 h in the solution at pH 2.8.

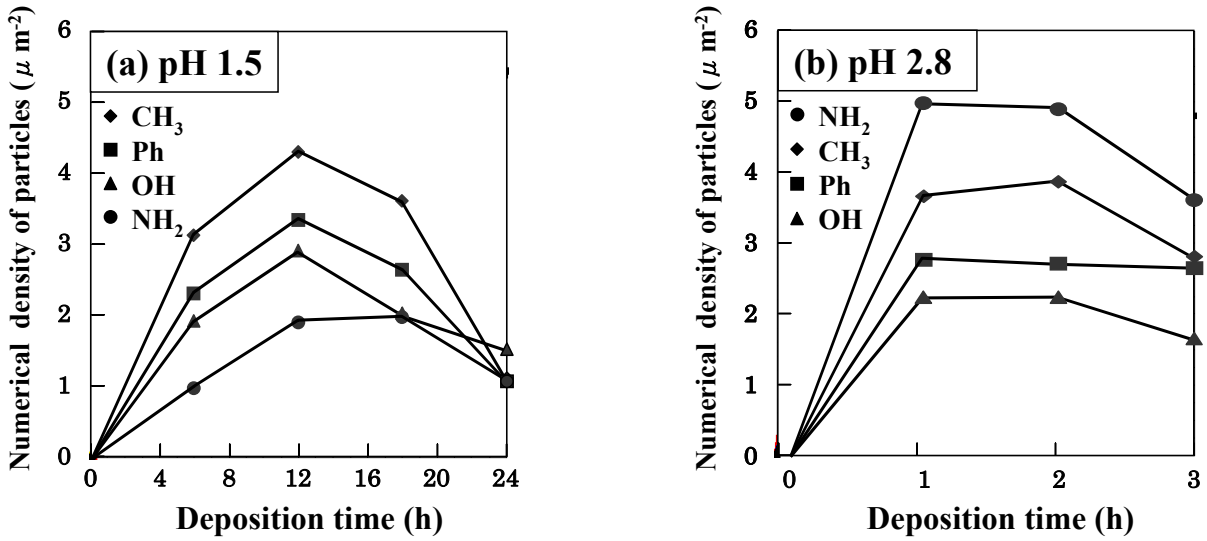

Figure 5. Numerical density of TiO_2 particles on SAMs which have phenyl, methyl, OH or amino groups in the solution at (a) pH 1.5 or (b) pH 2.8 as a function of deposition time.

Deposition processes in solutions at pH 1.26, 1.72, 2.22 or 3.75 were further studied, but no marked difference in deposition behavior was observed. The dissimilarity in either zeta potential or hydrophobicity of SAMs showed no salient difference in deposition behavior in our solution.

Crystal-axis orientation of TiO_2 thin film. The growth process of TiO_2 thin films and the crystal-axis orientation changes were investigated using an X-ray diffractometer (XRD; RAD-C, Rigaku) with CuKα radiation (40 kV, 30 mA) and Ni filter plus a graphite monochromater. Deposited films on all SAMs showed XRD patterns of anatase TiO_2 after 24 h at pH 1.5 or after 4 h at pH 2.8. XRD patterns showed the same tendency regardless of the type of SAM, and intensities of (004) and (105) peaks on all SAMs increased with deposition time faster than other peaks (Fig. 6). The degree of crystal-axis orientation (f) was evaluated using the Lotgering method[41] taking into account the following diffraction peaks: (101) = 25.3, (004) = 37.8 °, (200) = 48.0 °, (105) = 53.9 °, (204) = 62.7 °, (116) = 68.8 °, (215) = 75.0 ° (Fig. 7).

$$f = \frac{P - P_0}{1 - P_0} \quad \cdots\text{(d)}$$

$$P = \frac{\sum I(00l)}{\sum I(hkl)} \quad \cdots\text{(e)}$$

P: calculated for the oriented sample

P_0: P for non-oriented sample (JCPDS card)

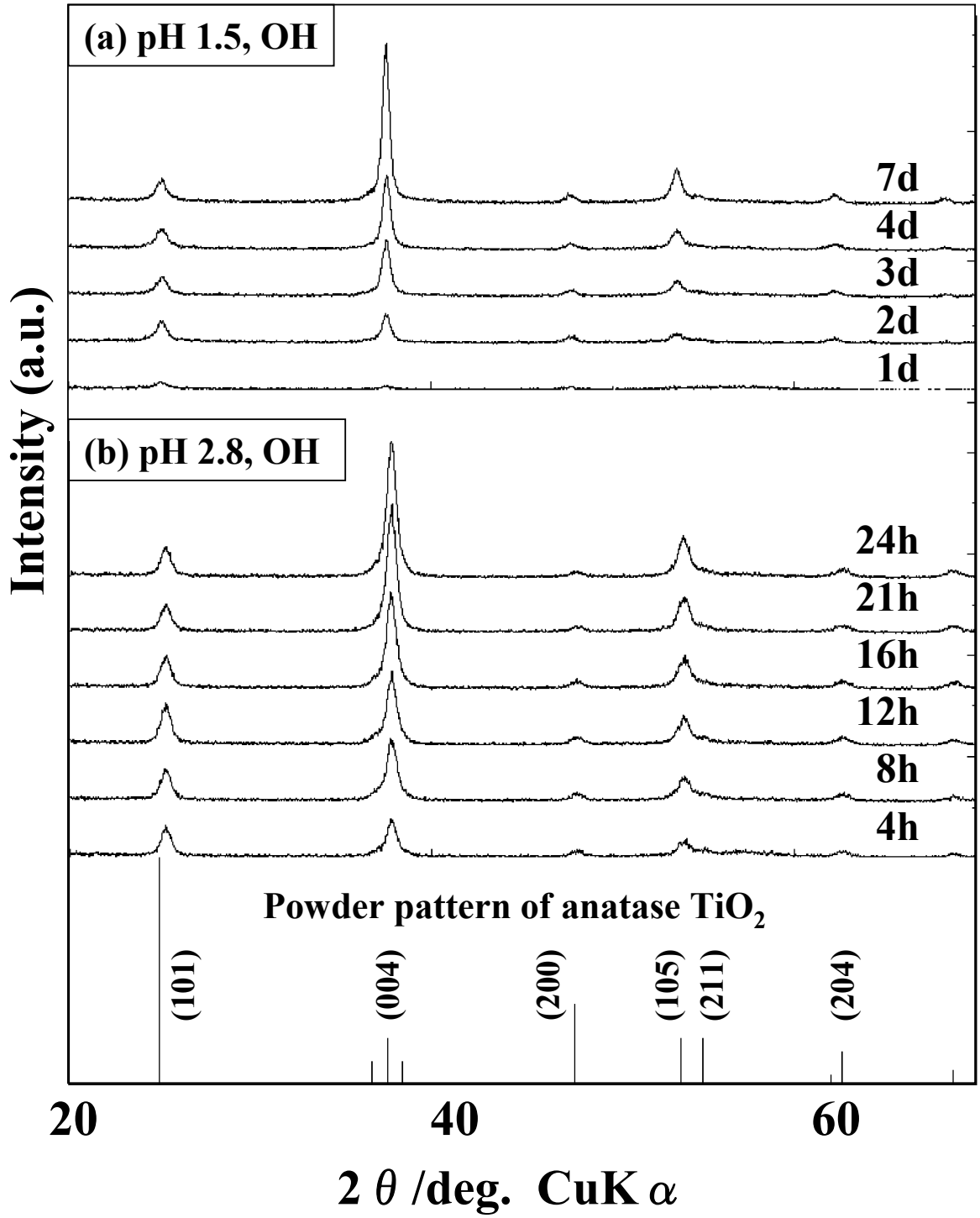

Figure 6. XRD patterns of anatase TiO_2 deposited onto OH groups in the solution at pH 2.8 as a function of deposition time. Randomly oriented powder pattern for anatase (JCPDS Card No. 21-1272) is shown for comparison.

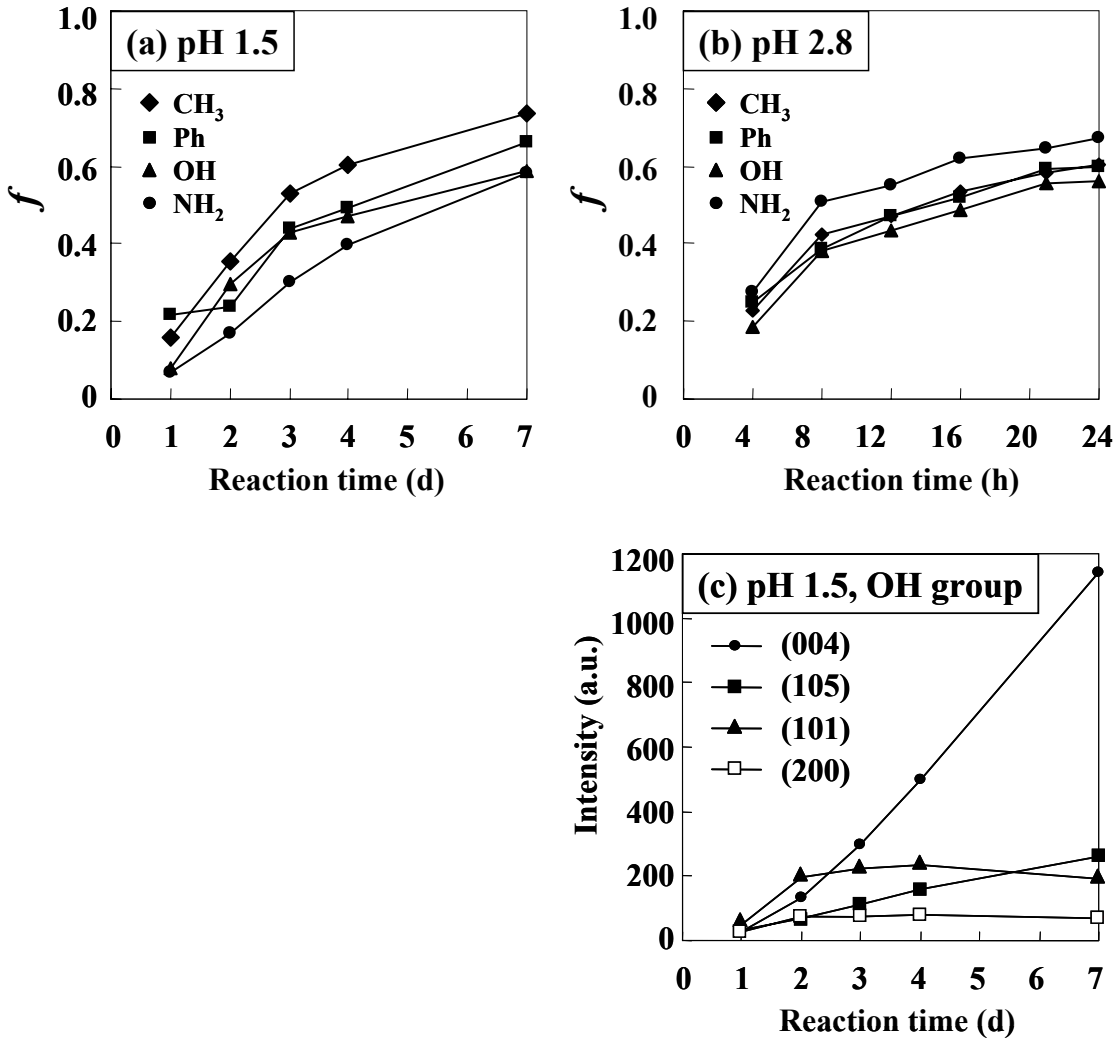

Figure 7. *f* (the degree of crystal-axis orientation) of anatase TiO_2 thin films deposited from the solution at (a) pH 1.5 or (b) pH 2.8, and (c) intensities of peaks as a function of reaction time (at pH 1.5, on OH groups).

The c-axis (00*l*) orientation of the film was enhanced by increasing the reaction time for all the kinds of SAMs and pH (Fig. 7a, b). This result suggests that the orientation of the film is determined not at the initial nucleation or deposition stage but at the film growth stage. The intensity of the (004) peak quickly increased but that of (105) increased only gradually with reaction time, and the intensities of the (101) and (200) peaks decreased after reaching their maxima regardless of the type of SAM or pH condition (Fig. 7c). Furthermore, the orientation of thin film deposited at pH 2.8 for 4 h was evaluated by a field emission scanning electron microscope (FE-SEM; JSM-6700F, point-to-point resolution 1 nm, JEOL Co., Ltd.) and a transmission electron microscope (TEM; JEM4010, 400 kV, point-to-point resolution 0.15 nm, JEOL Co., Ltd.). The cross section profile of TiO_2 thin films showed columnar morphology (Fig. 8). However, the columns were not clearly identified compared with the needle-like morphology of TiO_2 thin films reported

recently[15-16]. This columnar morphology is consistent with XRD measurement which showed weak c-axis orientation (Fig. 6, pH 2.8, 4 h). Figure 9 shows a TEM micrograph and electron diffraction pattern for the cross section profile of a TiO_2 thin film. Many small crystals of anatase TiO_2 were observed throughout the thin film. The electron diffraction pattern also showed weak orientation of anatase TiO_2 crystals.

These observations firmly indicate that TiO_2 particles whose c-axes were perpendicular to the substrate surface may have grown faster than other crystals. Hence, the diffraction intensities of crystal planes almost perpendicular to the c-axis such as (004) and (105) increased with deposition time (Fig. 7). These particles then consumed other particles whose c-axis was far from perpendicular to the substrate, thus lowering the diffraction intensities of crystal planes such as (101) and (200).

This phenomenon is plausible if the (00l) surface of an anatase crystal possesses the lowest energy compared to other crystallographic surfaces. However, the (002) surface has a high Gibbs free energy and the (110) plane has the lowest Gibbs free energy.[17] In general, the crystal plane with the lowest Gibbs free energy will grow preferentially, that is, the preferred orientation is the one having the lowest surface free energy. Hence, the preferred orientation should be (110) in the condition without any influence on crystal orientation in which atomic diffusion is more significant and the preferred orientation is affected more by thermodynamic factors. From these facts, the crystal growth of TiO_2 is considered to be controlled by some other factors.

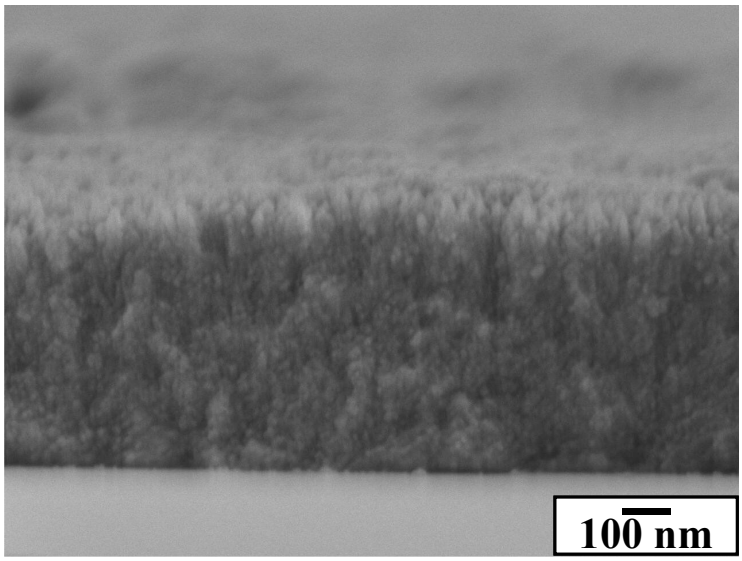

Figure 8. FE-SEM micrograph for cross section profile of TiO_2 thin film deposited at pH 2.8.

De Guire *et al.*[18] suggested that the selective adsorption of ions occurs on specific surfaces of anatase crystals. Oriented films do not always need oriented nucleation. The film can have an oriented fiber structure if crystals grow anisotropically. Preferential adsorption of ionic or polymeric species from the solution onto

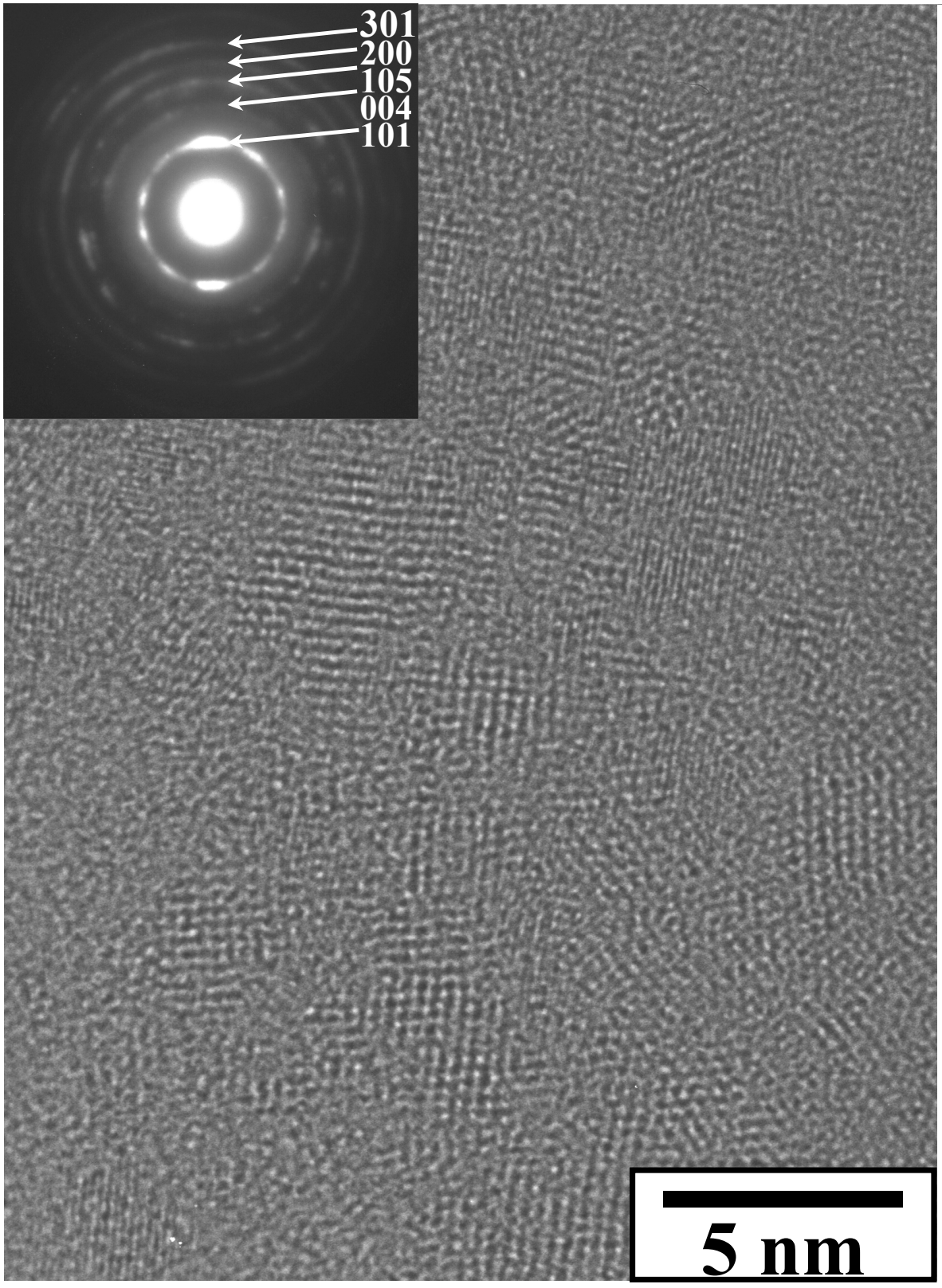

Figure 9. TEM micrograph and electron diffraction pattern for cross section profile of TiO_2 thin film deposited at pH 2.8.

certain crystallographic faces induces anisotropic growth. The elongated growth tendency of the crystals shown in Fig. 8 indicates that such growth anisotropy exists in our films. Additionally, the growth and crystallinity of anatase were discussed based on a systematic study of LPD TiO_2 films.[18] Growth via attachment of particles is usually associated with high growth rate, but also high roughness and reduced crystallographic orientation. However, De Guire *et al.* concluded that our method[21,30] provides anatase TiO_2 thin films with a high growth rate, high crystallinity and the smoothest surfaces in their comparative experiments.[18]

The adsorption of anions to anatase surfaces and its influence on preferred orientation were discussed by Yamabi and Imai.[15-16] The anatase TiO_2 films deposited from $TiOSO_4$ solution containing urea and from TiF_4 solution were composed of fine needles perpendicular to the substrate. The selective adsorption of coexisting species, such as SO_4^{2-} and F^-, on specific surfaces parallel to the c-axis inhibits the crystal growth perpendicular to the c-axis. In contrast, a randomly oriented uniform film consisting of fine spherical crystallites with diameters of 10–20 nm was deposited from the $TiOSO_4$ solution without urea.[15] A high reaction rate compared with $TiOSO_4$ solution containing urea[15] or TiF_4 solution[16] induces the random orientation of spherical particles.

Likewise, many kinds of anions, such as F^-, BO_3^{3-}, BF_4^- or TiF_6^{2-}, were included in our solution and these would adsorb to the surfaces parallel to the c-axis, inhibiting the growth in the direction perpendicular to the c-axis. The anatase crystals probably grow in the c-axis direction. The initial nuclei which have c-axes parallel to the substrate cannot grow fast because of the presence of neighboring particles, but in contrast, the particles which have c-axes perpendicular to the substrate can grow fast in the direction perpendicular to the substrate. Particles probably grow in the direction perpendicular to the substrate and give rise to columnar morphology as shown in Fig. 8 a, which would have caused the high degree of orientation of the (00l) plane perpendicular to the substrate.

Conclusions

The nucleation and growth process of anatase TiO_2 on several kinds of SAMs in an aqueous solution has been evaluated in detail. Homogeneously nucleated TiO_2 particles and amino groups of SAM showed negative or positive zeta potential in the solution, respectively. The adhesion of TiO_2 particles to the amino group surface by attractive electrostatic interaction would cause rapid growth of TiO_2 thin films in the supersaturated solution at pH 2.8. On the other hand, TiO_2 was deposited on SAMs without the adhesion of TiO_2 particles regardless of the type of SAM in the solution at pH 1.5 whose supersaturation degree was low due to high concentration of H^+. Furthermore, the crystal-axis orientation of films deposited on substrates

was shown to be improved by changing the reaction time. TiO_2 crystals whose c-axes were perpendicular to the substrate surface may have grown faster than other crystals possibly because of the selective adsorption of the coexisting species, such as F^-, BO_3^{3-}, BF_4^- or TiF_6^{2-}, on specific surfaces parallel to the c-axis. The growth via attachment of particles is usually associated with high growth rate, but also high roughness and reduced crystallographic orientation. However, our method avoided this compromise, yielding a high growth rate as well as partial crystallographic orientation and smooth surfaces.

References

(1) Furlong, D. N.; Parfitt, G. D. *J. Colloid Interface Sci.* **1978**, *65(3)*, 548-554.

(2) Larson, I.; Drummond, C. J.; Chan, D. Y. C.; Grieser, F. *J. Am. Chem. Soc.* **1993**, *115*, 11885.

(3) Wiese, G. R.; Healy, T. W. *J. Colloid Interface Sci.* **1975**, *51*, 427-433.

(4) Yotsumoto, H.; Yoon, R. H. *J. Colloid Interface Sci.* **1993**, *157*, 426.

(5) Morimoto, T.; Sakamoto, M. *Bull. Chem. Soc. Jpn.* **1964**, *37(5)*, 719-723.

(6) Parfitt, G. D.; Wharton, D. G. *J. Colloid Interface Sci.* **1972**, *38(2)*, 431-439.

(7) Zhu, P. X.; Ishikawa, M.; Seo, W. S.; Koumoto, K. *J. Biomed. Mater. Res.* **2002**, *59*, 294-304.

(8) Gun J.; Sagiv, J. *J. Colloid Interface Science* **1986**, *112*, 457-472.

(9) McGovern, M. E.; Kallury, K. M. R.; Thompson, M. *Langmuir* **1994**, *10*, 3607-3614.

(10) Duchet, J.; Chabert, B.; Chapel, J. P.; Gerard, J. F.; Chovelon, J. M.; Jaffrezic-Renault, N. *Langmuir* **1997**, *13*, 2271-2278.

(11) Dressick, W. J.; Chen, M-S.; Brandow, S. L. *J. Amer. Chem. Soc*. **2000**, *122*, 982-983.

(12) Dressick, W. J.; Chen, M-S.; Brandow, S. L.; Rhee, K. W.; Shirey, L. M.; Perkins, F. K. *Appl. Phys. Lett.* **2001**, *78*, 676-678.

(13) Dressick, W. J.; Nealey, P. F.; Brandow, S. L. *Proc. SPIE* **2001**, *4343*, 294-305.

(14) Lotgering, F. K.; *J. Inorg. Nucl. Chem.* **1959**, *9*, 113-123.

(15) Yamabi, S.; Imai, H. *Chem. Mater*. **2002**, *14*, 609-614.

(16) Shimizu, K.; Imai, H.; Hirashima, H.; Tsukuma, K. *Thin Solid Films* **1999**, *351*, 220-224.

(17) Leng, Y. X.; Huang, N.; Yang, P.; Chen, J. Y.; Sun, H.; Wang, J.; Wan, G. J.; Tian, X. B.; Fu, R. K. Y.; Wang, L. P.; Chu, P. K. *Science and Coating Technology* **2002**, *156*, 295-300.

(18) Pizem, H.; Sukenik, C. N.; Sampathkumaran, U.; McIlwain, A. K.; De Guire, M. R. *Chem. Mater.* **2002**, *14*, 2476-2485.

(19) Koumoto, K.; Seo, S.; Sugiyama, T.; Seo, W. S.; Dressick, W. J. *Chem. Mater.* **1999**, *11(9)*, 2305.

(20) Masuda, Y.; Sugiyama, T.; Koumoto, K. *J. Mater. Chem.* **2002**, *12(9)*, 2643-2647.